ORIGINAL ARTICLE

# Preparation of the 5-(4-((4-[18F] fluorobenzyl) oxy)-3-methoxybenzyl) pyrimidine-2, 4-diamine as a radioligand for positron emission tomography scanning of the tyrosine kinase b/C receptor

Seyyed Hossein Hassanpour[1]*, Alireza Doroudi[2], Seyyedeh Zeinab Karami[3]

**Pakistan Journal of Nuclear Medicine**
Volume 12(1):37–48
https://doi.org/10.24911/PJNMed.175-1631138374



Pakistan Journal of Nuclear Medicine is the official journal of Pakistan Society of Nuclear Medicine

## ABSTRACT

**Objective**: The present research describes a new radiosynthesis of 5-(4-((4-[$^{18}$F]fluorobenzyl)oxy)-3-methoxybenzyl)pyrimidine-2,4-diamine as a potential radioligand for colony-stimulating factor 1 receptor (CSF-1R) and tyrosine kinase B/C (TrkB/C) neuroreceptors.

**Methods:** Radiofluorination of a boronic acid precursor followed by thermal deprotection of Boc-protecting groups avoided acid-catalyzed protodeboronation in 8.7 ± 2.8% radiochemical yield.

**Results:** Competitive autoradiographic binding research indicated a high unspecific binding, and that binding to TrkB/C could be blocked while binding to CSF-1R was not. In a rat model, a positron emission tomography (PET) scan indicated a moderate brain uptake and slow clearance rate.

**Conclusion:** Moreover, the poor pharmacokinetic features of 5-(4-((4-[$^{18}$F]fluorobenzyl)oxy)-3-methoxybenzyl)pyrimidine-2,4-diamine prevented its utilization as a PET radioligand in brain scanning, but 1-pot synthesis (which is a strategy to improve the effectiveness of the chemical reaction occurring by the use of copper, $^{18}$F-fluorination, and Boc deprotection) is an approach to the radio-synthesis of PET tracers (which are sensitive to acid).

**Keywords:** Tyrosine kinase, colony-stimulating factor 1 receptor, $^{18}$F, positron emission tomography.

**Received:** 08 September 2021 **Revised:** XXXX **Accepted:** 10 March 2022
**Correspondence to:** Seyyed Hossein Hassanpour,
*Young Researchers and Elite Club, Yassoj Branch, Islamic Azad University, Yasooj, Iran.
**Email:** Dr.hossein1366@yahoo.com
*Full list of author information is available at the end of the article.*

## Background

Researchers have considered tyrosine kinase (Trk) receptors as one of the families of 3 receptor tyrosine kinases that are stimulated by 1 or more four neurotrophins, involving brain-derived neurotrophic factor (BDNF), neurotrophins 3 and 4 (NT-3 and NT-4), and nerve growth factor. Furthermore, the survival of various cells, outcome neural precursors, proliferation or rapid growing, dendrite and axon growth, the composition according to a pattern, and activities and production of functionally significant proteins (such as ion channel and neurotransmitter receptors) are regulated by neurotrophin signaling via these receptors. On the other hand, in the adult nervous system, synaptic plasticity and strength are regulated by Trk receptors [1]. By binding to cognate neurotrophin ligands, Trk receptors are actuated and experience dimerization with an unliganded monomeric shape assumed to be stable in the phosphorylated dimeric condition [2], which is of crucial importance and regulates the downstream intracellular biochemical actions of neurotrophins and respective receptors [3,4]. In fact, TrkB is one of the single-pass type 1 membrane proteins that can be incorporated into endosomes upon ligand binding. Downregulation of the Trk receptor was seen in some central nervous system (CNS) dysfunctions such as Alzheimer disease (AD) and other similar mental-related disorders [5]. Colony-stimulating factor 1 receptor (CSF-1R) was considered to be one of the cell surface proteins encoded by the *CSF1R* gene (also called C-FMS) in humans [6]. This protein is one of the receptors for a cytokine known as a CSF. In fact, the encoded protein is a receptor of the Trk membrane and

thus can be categorized as a CSF1/platelet-derived growth factor family, which belongs to the tyrosine-protein kinase [7,8].

Researchers have seen greater CSF-1R in microglia in AD following damage to the brain. Higher levels of receptor expression result in greater activity of microglia [9]. Thus, CSF-1R inhibition offers an opportunity to survey neurodegenerative diseases due to microglia [10]. Imaging equipment is being used for a major review of CSF-1R action and Trk in the *in vivo* brain and estimation of the outcome of receptor-mediated treatments. *Ex vivo* post-mortem analyses or invasive techniques are exclusively applied to analyze, investigate, and quantify Trk receptors in neurodegenerative illnesses and cancers. Moreover, more information should be collected on prototypical radioligands, such as [$^{18}$F]TRACK and [$^{11}$C]-(*R*)-IPMICF16, which show a moderate brain uptake in humans, to understand if they are suitable for clinical neuroimaging, and if they can supply well-founded CNS TrkB/C estimates or sufficiently identify declines in the density of the receptor.

Although tracers have the highest level of brain discernment and volume of distribution values, or binding potential will be favorable for the spatial and temporal assessments of Trk expression under situations such as AD, these novel tracers were advantageous in conditions wherein Trk was overexpressed; for instance, in multiple human cancers in CNS and PNS. Continual expansion of positron emission tomography (PET) radiotracers for imaging neuroinflammation leads to promising, noninvasive strategies that may result in initial diagnosis, tracking disease expansion, and helping in creating a reasonable design and clinical evaluation of the patient's response to treatment interventions [11]. As a result, a PET agent would be a worthwhile option to develop new treatment choices for neuroinflammation, specifically those that target CSF-1R and prepare a noninvasive, iterable read out in patients and measure the target's involvement [12]. Primary preclinical PET scanning in rodents and nonhuman primates demonstrated a lower brain signal of [$^{11}$C] AZ683. In general, PET imaging outputs propose that the association of CSF-1R imaging with neuroinflammation using [$^{11}$C]AZ683 may be difficult, and it focused that the increased affinity, acceptable selectivity, and good drug-like characteristics would not guarantee that this compound would become an acceptable radiopharmaceutical for *in vivo* brain PET. Researchers have also found the potential use of [$^{11}$C]AZ683 for imaging peripheral CSF-1R to determine its role in brain inflammation [13]. The first compound, which simultaneously suppresses Trk/CSF-1R receptors and was thought to be a radiotracer for these 2 receptors, is 5-(4-((4-[$^{18}$F]fluorobenzyl) oxy)-3-methoxybenzyl)pyrimidine-2,4-diamine [14].

Furthermore, 5-(4-((4-[$^{18}$F]fluorobenzyl)oxy)-3-methoxybenzyl)pyrimidine-2,4-diamine, as a type II tyrosine kinase inhibitor (TKI), has better pharmacokinetic properties than radiotracers, which are type I TKIs. The number of procedures for incorporating fluorine into (hetero)-arenes has increased since 10 years ago because such structural motifs were generally observed in the pharmaceutical options to elevate metabolic robustness [15]. The main purpose of this study was to investigate the effective radiolabeling of the $^{18}$F-fluorinated derivative of dual inhibitor GW2580. In the next step, this inhibitor was used as a candidate for PET detection to identify and image 2 neuroreceptors (tropomyosin receptor kinase and CSFR) involved in the pathophysiology of neurodegenerative diseases.

## Material and Methods

### *Materials*

All chemical materials were purchased from Merck or Fluka. SPSS 20 (SPSS Inc, Chicago, IL). The chemicals and solvents were of the highest purity and analytical grade and used without further purification. All reactions were monitored with analytical reverse-phase high-performance liquid chromatography (RP-HPLC) on a JASCO 880-PU intelligent pump HPLC system (Tokyo, Japan) and NMR and high-resolution mass spectrometry (HRMS). The PET images were acquired using a CTI Concorde R4 microPET scanner for small animals (CTI, Siemens, Munich, Germany). Anesthesia was first induced using isoflurane at 5% with a 2- to 3-l/minute oxygen flow and then maintained for the duration of the scan at 1.5%-2.5% isoflurane with a 0.8-l/minute oxygen flow. Male Wistar rats were obtained from the Research Center and Experimental Animal House of Tehran University of Medical Sciences (TUMS) for microPET imaging experiments. The autoradiography used in this study was performed according to the Biospace Lab Company and BetaIMAGER model. The reagents were purchased from commercial centers and utilized with no more purification unless otherwise specified. Flash column chromatography was performed by applying silica 60 Å (particle size 40-63 µm) as the stationary phase.

Compounds were visualized under UV light; compounds that could not be visualized by UV light were treated with $KMnO_4$ stain. All $^{1}$H, $^{13}$C, and $^{19}$F NMR spectra were documented on a 2-channel Bruker 400 or 500 MHz AVIIIHD device with an Ascend magnet equipped with a Bbfo Plus Smartprobe (Bruker Corporation) at a constant temperature of 298 K. COSY, DEPT, HSQC, and HMBC experiments were applied to aid structural determination and spectral assignment. Chemical shifts ($\delta$) are described in millions (ppm) and compared based on the maximum residual solvent. Coupling constants (*J*) are described in hertz (Hz) to the closest 0.5 Hz. Standard abbreviations showing multiplicities are as follows: br, broad; d, doublet; m, multiplet; p, pentet; q, quartet; s, singlet; and t, triplet.

HRMS data were collected by a Bruker Maxis Impact Q-TOF by ESI-MS in a positive or negative ionization mode. Radiosynthesis and HPLC purifications were performed using an automated radiosynthesis unit (Scintomics, GRP), which had a semi-preparative HPLC module (Knauer) fitted with a Phenomenex LUNA C18 column (100 Å, 250 × 10 mm, 10 µm). Analytical HPLC was conducted by an Agilent 1200 series HPLC by applying a Phenomenex Prodigy ODS-3 column (250 × 4.6 mm, 10 µm). Outputs were controlled with UV and radioactivity detectors.

## Experimental section and methods

As a type II TKI, this PET tracer candidate was hypothesized to display improved pharmacokinetics compared to Trk tracers based on type I inhibitors due to reduced endogenous competition with ATP. As a type II TKI, this PET tracer candidate was hypothesized to display improved pharmacokinetics compared to Trk tracers based on type I inhibitors due to reduced endogenous competition with ATP. Notably, GW2580 exhibits one of the most specific kinase inhibition profiles among known kinase inhibitors (no supplementary inhibition of other kinases with Kd <3 µM), which, when considering PET imaging, represents an advantageous target selectivity.

## Synthesis

### Synthesis of intermediate

As indicated in Figure 1, boronic acid pinacolate is one of the necessary materials for making 5-(4-((4-[$^{18}$F] fluorobenzyl)oxy)-3-methoxybenzyl)pyrimidine-2,4-diamine and synthesized as follows: The reaction of 1-(bromomethyl)-4-iodobenzene with 4-hydroxy-3-methoxybenzaldehyde (vanillin) to form compound 1, and consecutive condensation with 3-morpholinopropionitrile. Then, the substitution of the morpholino group with vanillin was performed. Finally, annulation with guanidine efficiency 4 was done. Then, diamino-pyrimidine moiety should be safeguarded using 4-dimethylaminopyridine (DMAP)-catalyzed putting in of 4 tert-butyl formate categories (5), which leads to subsequent Miyaura borylation (6) and ultimate labeling reaction to continue no intervention with free amines.

Compound 6, as a precursor to producing 5-(4-((4-[$^{18}$F]fluorobenzyl)oxy)-3-methoxybenzyl)pyrimidine-2,4-diamine and another by-product (BOMPyD), was synthesized with 38% efficiency. This compound was synthesized by applying para-iodobenzyl bromide with the reactions noted in Figure 1. To separate fluoride compounds-$^{18}$F from target [$^{18}$O] $H_2O$, we applied the "minimalistic method," which was first introduced by Zischler et al. [16]. In brief, [$^{18}$F] F−/$H_2O$ was moved through a Sep-Pak Accell plus QMA Carbonate plus Light cartridges (46 mg, Waters), which contains a carbonate counter ion and a silica-based, hydrophilic robust anion exchanger. Then, we utilized 3 ml of anhydrous methanol (MeOH) to prevent the impact of water. $^{18}$F-fluoride was eluted by applying 450 µl, 1 mg/ml, MeOH in the opposite direction to tetraethylammonium bicarbonate solution. Then, 500 µl of pure and fresh MeOH was poured into a reaction vial where reactions take place. Afterward, we deleted the solvent during decreasing pressure at 90°C. The procedure was performed under argon gas.

To provide the best and most efficient radiolabeling, a solution of compound 6 (8.6 mg, 10 µmol) and tetrakis (pyridine) copper (II) bis (trifluoromethanesulfonate) in a mixture of dimethylacetamide (DMA)/1-butanol (1-BuOH) solvent (2:1, 450 lL total) were poured into dried [$^{18}$F] TEAF/$TEAHCO_3$. Then, the obtained mixed solvent was gradually heated to 110°C, and then the temperature rose to 130°C. The advancement of the reaction was controlled using radio-TLC. HPLC undertook the purification with the following specifications: brand:

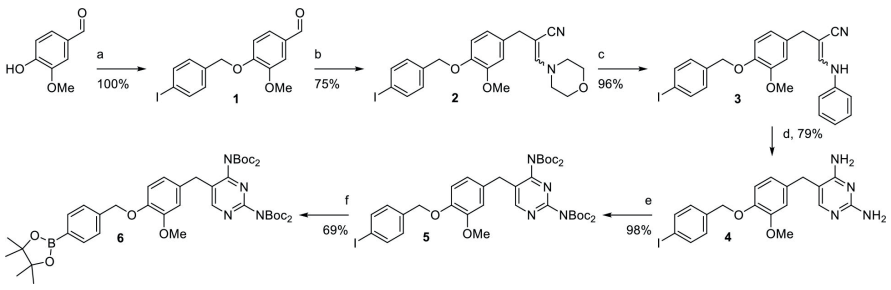


***Figure 1.*** *Synthesizing precursor 6. under conditions of (a) Caesium carbonate, p-iodo- bromomethylbenzene (Solvent): Acetonitrile (methyl cyanide), Heating the chemical reaction for a certain period of time and continuously cooling the vapor produced by using a condenser to become a liquid , (b) 3-morpholino-propionitrile, Sodium hydride (Solvent): dimethylsulfoxide, 75°C, (c) Benzenamine · Hydro chloride,(Solvent): 2-propanol, 40°C, (d). Iminomethanediamine (HNC(NH2)2) · hydrochloride, Sodium methoxide, (Solvent): ethanol, Heating the chemical reaction for a certain period of time and continuously cooling the vapor produced by using a condenser to become a liquid (reflux), (e) di-tert-butyl dicarbonate, 4-dimethylaminopyridine,(Solvent): tetrahydrofuran, (f) $B_2pin_2$, Pd(dppf)Cl2, KOAc, (Solvent): dimethyl sulfoxide as dipolar aprotic solvent, 80°C.*

Phenomenex Luna; stationary phase: C18 (2); the size of the particle: 10 µm; the size of the pores: 100 Å; length: 250 mm; internal diameter: 10 mm.

The mobile phase was the mixture of acetonitrile/methyl cyanide (MeCN) and 20 mM aqueous $NaH_2PO_4$ (30:70) with a flow rate of 4 ml/minute. When the radiotracer was provided, the formulation was done in 10% ethanol, and its stability was evaluated by radio-HPLC analysis. The column specifications were as follows: brand: Prodigy; phase: ODS-3; size of the particle: 5 µm; size of the pores: 100 Å; length: 100 mm; internal diameter: 4.6 mm; stationary phase: C18; solid support: completely porous silica; format: column; separation mode: reversed phase; recommended use: small molecules.

The mobile phase was the mixture of MeCN and 0.1% aqueous trifluoroacetic acid (TFA) with a flow rate of 0.7 ml/minute (Figure 2).

## $^{18}F$ Synthesis

*4-((4-Iodobenzyl)oxy)-3-methoxybenzaldehyde: Compound 1*

To obtain compound 1, 0.543 g of 4-iodo-benzyl bromide (1.82 mmol), 0.306 g of vanillin (2.01 mmol), and 0.894 g of $Cs_2CO_3$ (2.74 mmol) were suspended in 18.5 ml MeCN in a 50-ml flask, which was fitted with a condenser. Then, the solvent was refluxed for 1 hour and then removed under decreased pressure, and the solids separated into water and ethyl acetate (EtOAc). The organic phase was rinsed once with brine. Then, it was dried using $Na_2SO_4$ and filtered; after decreasing pressure, the solvent was removed. Afterward, flash chromatography (silica, 20% EtOAc/petroleum ether) was used to purify the obtained product, yielding the product as 0.672 mg of white, crystalline solid in quantitative yield. $^1H$ NMR [500 MHz,

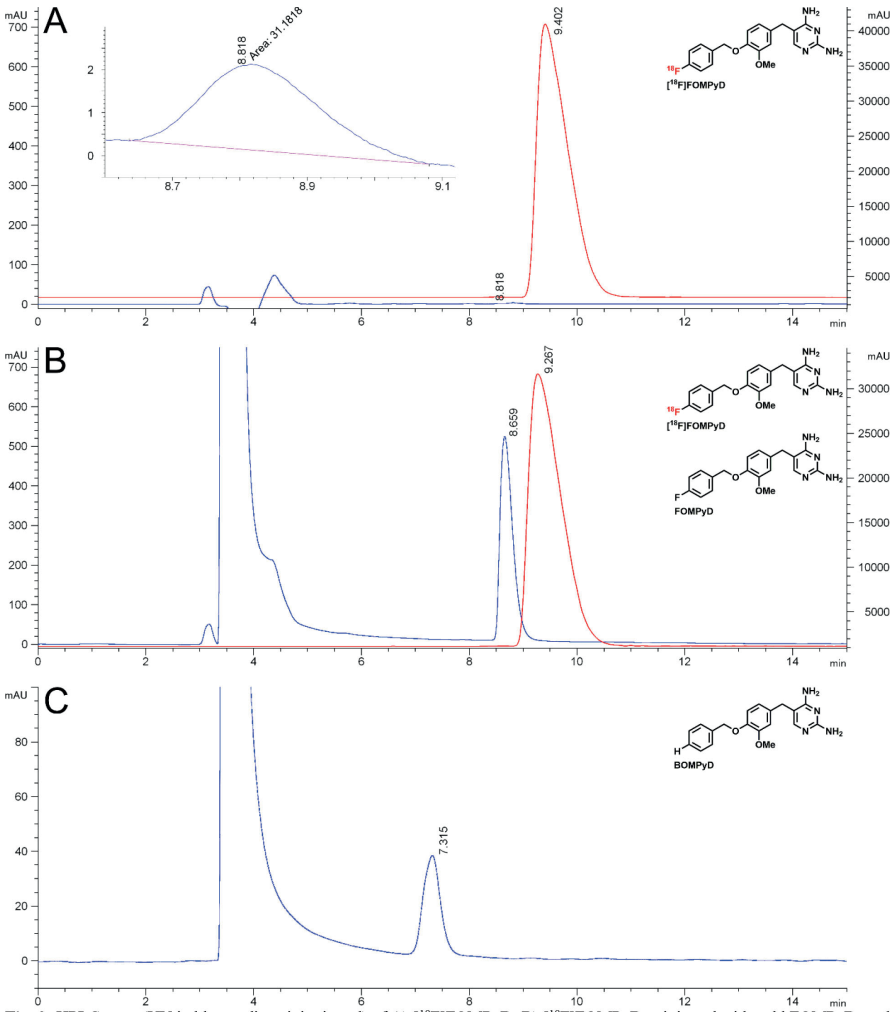


***Figure 2.*** *HPLC trace (UV in blue, radioactivity in red) of (A) [$^{18}F$]FOMPyD, (B) [$^{18}F$]FOMPyD coinjected with cold FOMPyD, and (C) protodeboronation side-product BOMPyD on a Phenomenex Prodigy ODS-3 column (250 × 4.6 mm, 10 µm), 40:60 MeCN:0.1% TFA, 0.7 ml·minute$^{-1}$, monitored at 210 nm. The solvent feature at 3.8 min is the DMSO matrix used for the standard cold injection.*

dimethylsulfoxide (DMSO)-$d_6$]: $\delta$ 9.84 (s, 1 H), 7.79-7.75 (m, 2 H), 7.53 (dd, $J$ = 8.2, 1.9 Hz, 1 H), 7.42 (d, $J$ = 1.9 Hz, 1 H), 7.29-7.25 (m, 2 H), 7.23 (d, $J$ = 8.3 Hz, 1 H), 5.19 (s, 2 H), 3.84 (s, 3 H). $^{13}$C NMR (126 MHz, DMSO-$d_6$) $\delta$ 191.4, 152.9, 149.4, 137.3, 136.2, 130.1, 129.9, 125.8, 112.7, 109.8, 94.2, 69.3, 55.6. HRMS (Atmospheric Pressure Chemical Ionization $^+$): m/z calcd for $C_{15}H_{14}IO_3$ ([M+H]$^+$): 368.9982; found: 368.9990.

## 2-(4-((4-Iodobenzyl)oxy)-3-methoxybenzyl)-3-morpholinoacrylonitrile: Compound 2

To obtain compound 2, 673 mg of compound 1 (1.8 mmol) and 247 µl of 4-morpholinopropionitrile were dissolved in 5 ml of DMSO in a Wheaton vial. Seventy-three milligrams of NaH (3.04 mmol; 60% dispersion in mineral oil, 0.3 eq.) was mixed. In the following, the suspension was heated with vigorous stirring to 70 °C for 30 minutes. Afterward, the reaction mixture was quenched into brine, and the obtained suspension was extracted 2× with EtOAc. The organic phase was separated, dried over $Na_2SO_4$, and filtered; after achieving declined pressure, the solvent was removed. To obtain the product as a 670-mg yellow solid in a 75% yield, flash chromatography (silica, 0%-50% EtOAc/petroleum ether) was used to purify the crude product. $^1$H NMR (500 MHz, DMSO-$d_6$): $\delta$ 7.77-7.72 (m, 2 H), 7.26-7.22 (m, 2 H), 6.93 (d, $J$ = 8.2 Hz, 1 H), 6.84 (d, $J$ = 2.0 Hz, 1 H), 6.78 (s, 1 H), 6.70 (dd, $J$ = 8.2, 2.0 Hz, 1 H), 5.02 (s, 2 H), 3.76 (s, 3 H), 3.61 (dd, $J$ = 5.7, 4.0 Hz, 4 H), 3.45-3.40 (m, 4 H), 3.26 (s, 2 H). $^{13}$C NMR (126 MHz, DMSO-$d_6$): $\delta$ 149.7, 149.0, 146.2, 137.2, 137.1, 133.4, 129.8, 121.7, 119.9, 113.9, 112.4, 93.8, 73.0, 69.3, 65.6, 55.6, 48.8, 37.9. HRMS(APCI+): m/z calcd for $C_{22}H_{24}IN_2O_3$ ([M+H]$^+$): 491.0826; found: 491.0838.

## 2-(4-((4-Iodobenzyl)oxy)-3-methoxybenzyl)-3-(phenylamino)acrylonitrile: Compound 3

To obtain compound 3, 670 mg of compound 2 (1.37 mmol) and 177 mg of aniline hydrochloride (1.36 mmol) were suspended in 5 ml isopropanol. In order to achieve reflux, the mixture was heated for half an hour. Then, it was put at room temperature. The flask was then cooled to −5°C for 30 minutes. Afterward, filtration was used to collect the precipitate in order to reach the target compound as 653 mg of off-white powder (96%) of sufficient purity for use in the following step: $^1$H NMR (500 MHz, DMSO-$d_6$): $\delta$ 9.10 (d, $J$ = 12.6 Hz, 1 H), 7.78-7.71 (m, 2 H), 7.61 (d, $J$ = 12.6 Hz, 1 H), 7.28-7.23 (m, 4 H,), 7.20-7.15 (m, 2 H), 6.95 (d, $J$ = 8.2 Hz, 1 H), 6.93-6.88 (m, 1 H), 6.90 (d, $J$ = 2.1 Hz, 1 H), 6.75 (dd, $J$ = 8.2, 2.0 Hz, 1 H), 5.02 (s, 2H), 3.76 (s, 3 H), 3.42 (s, 2 H). $^{13}$C NMR (126 MHz, DMSO-$d_6$): $\delta$ 149.1, 146.2, 142.4, 141.8, 137.2, 132.9, 129.9, 129.2, 121.2, 120.1, 119.5, 115.2, 113.9, 112.5, 93.8, 80.7, 69.4, 55.6, 36.0. HRMS(ESI+): m/z calcd for $C_{24}H_{21}IN_2NaO_2$ ([M+Na]$^+$): 519.0540; found: 519.0534.

## 5-(4-((4-Iodobenzyl)oxy)-3-methoxybenzyl)pyrimidine-2,4-diamine: Compound 4

To obtain compound 4, 653 mg of compound 3 (1.3 mmol) and 188 mg of guanidine hydrochloride (1.96 mmol) were suspended in 12 ml EtOH in a 25-ml round bottom flask. Furthermore, 4.0 ml 0.5 M sodium methoxide (NaOMe) solution (2 mmol) was mixed with stirring, and the obtained mixture was fitted using a condenser. Then, it was stirred at reflux for 20 hours, following maintenance at 5°C for 30 minutes, and the resulting precipitate was then collected by filtration and washed with cold EtOH. Flash chromatography [silica, 0%-10% MeOH/dichloromethane (DCM)] was applied to purify the crude product (silica, 0%-10% MeOH/DCM) and isolated as 480 mg of white powder in a 79% yield. $^1$H NMR (500 MHz, DMSO-$d_6$): $\delta$ 7.76-7.72 (m, 2 H), 7.46 (s, 1 H), 7.25-7.21 (m, 2 H), 6.91-6.87 (m, 2 H), 6.67 (dd, $J$ = 8.2, 2.0 Hz, 1 H), 6.19 (s, 2 H), 5.81 (s, 2 H), 4.99 (s, 2 H), 3.73 (s, 3 H), 3.52 (s, 2 H). $^{13}$C NMR (126 MHz, DMSO-$d_6$): $\delta$ 162.3, 161.6, *154.3, 149.0, 145.8, 137.2, 137.1, 133.0, 129.8, 120.2, 113.9, 112.9, 106.2, 93.8, 69.4, 55.5, 32.2; *only observed in HSQC/HMBC spectra. HRMS(ESI+): m/z calcd for $C_{19}H_{20}IN_4O_2$ ([M+H]$^+$): 463.0625; found: 463.0619.

## Di-tert-butyl(5-(4-((4-iodobenzyl)oxy)-3-methoxybenzyl)pyrimidine-2,4-diyl)bis((tert-butoxycarbonyl)carbamate): Compound 5

To obtain compound 5, 103 mg of compound 4 (0.22 mmol), 490 mg of di-tert-butyl dicarbonate ($Boc_2O$; 2.24 mmol), and 5.5 mg of DMAP (0.045 mmol) were suspended in 3.5 ml degassed tetrahydrofuran (THF) in a Wheaton vial. Then, the solvent was stirred under argon for 72 hours until it was judged complete by TLC (40% EtOAc/petroleum ether); then, the volatiles were deleted under declined pressure. Flash chromatography (silica, 0%-50% EtOAc/petroleum ether) was used to purify the crude product, yielding 189 mg of pure product in a 98% yield. $^1$H NMR (500 MHz, DMSO-$d_6$): $\delta$ 8.90 (s, 1 H), 7.77-7.70 (m, 2 H), 7.25-7.18 (m, 2 H), 6.91 (d, $J$ = 8.2 Hz, 1 H), 6.80 (d, $J$ = 2.1 Hz, 1 H), 6.61 (dd, $J$ = 8.3, 2.0 Hz, 1 H), 5.00 (s, 2 H), 3.79 (s, 2 H), 3.72 (s, 3 H), 1.38 (s, 18 H), 1.27 (s, 18 H). $^{13}$C NMR (126 MHz, DMSO-$d_6$): $\delta$ 161.7, 159.0, 156.2, 150.3, 149.1, 149.0, 146.3, 137.2, 137.0, 130.4, 129.8, 120.7, 113.8, 113.0, 93.8, 83.3, 83.2, 69.2, 55.3, 33.1, 27.3, 27.1. HRMS (ESI+): m/z calcd for $C_{39}H_{52}IN_4O_{10}$ ([M+H]$^+$): 863.2723; found: 863.2703.

## Di-tert-butyl (5-(3-methoxy-4-((4-(4,4,5,5-tetramethyl-1,3,2-dioxaborolan-2-yl)benzyl)oxy)benzyl)pyrimidine-2,4-diyl)bis((tert-butoxycarbonyl)carbamate): Compound 6

To obtain compound 6, 98 mg of compound 5 (0.11 mmol), 35 mg bis(pinacolato)diboron ($B_2pin_2$; 0.137

mmol), 17 mg of [1,1′-bis(diphenylphosphino)ferrocene] dichloropalladium(II) [Pd(dppf)$Cl_2$] (0.023 mmol), and 22 mg of potassium acetate (KOAc; 0.224 mmol) were sealed in a vial. The vial was then purged with argon, and 2.5 ml degassed DMSO was added. The vial was heated to 80°C with stirring for 18 hours, followed by cooling at room temperature. Afterward, the solvent was diluted with EtOAc, washed twice with brine, and then dried using $Na_2SO_4$. The volatiles were then removed after achieving declined pressure, and flash chromatography (silica, 0%−40% EtOAc /petroleum ether) was applied to purify the crude product to yield the product as 68 mg in a 69% yield. $^1$H NMR (500 MHz, DMSO-$d_6$): $\delta$ 8.90 (s, 1 H), 7.69-7.62 (m, 2 H), 7.44-7.38 (m, 2 H), 6.90 (d, $J$ = 8.3 Hz, 1 H), 6.80 (d, $J$ = 2.1 Hz, 1 H), 6.60 (dd, $J$ = 8.2, 2.1 Hz, 1 H), 5.07 (s, 2 H), 3.79 (s, 2 H), 3.73 (s, 3 H), 1.38 (s, 18 H), 1.28 (s, 12 H), 1.27 (s, 18 H). $^{13}$C NMR (126 MHz, DMSO-$d_6$): $\delta$ 161.7, 159.0, 156.2, 150.3, 149.1, 149.0, 146.4, 140.6, 134.5, 130.3, 129.8, 126.8, 120.7, 113.8, 113.0, 83.6, 83.3, 83.1, 69.7, 55.3, 27.3, 27.1, 24.6. HRMS(ESI+): m/z calcd for $C_{45}H_{64}BN_4O_{12}$ ([M+H]$^+$): 863.4608; found: 863.4578.

### 5-(4-((4-Fluorobenzyl)oxy)-3-methoxybenzyl) pyrimidine-2,4-diamine: FOMPyD

The synthetic procedure was previously reported in reference 2. $^1$H NMR (500 MHz, DMSO-$d_6$): $\delta$ 7.49-7.44 (m, 2 H), 7.46 (s, 1 H), 7.23-7.17 (m, 2 H), 6.92 (d, $J$ = 8.2 Hz, 1 H), 6.89 (d, $J$ = 2.0 Hz, 1 H), 6.68 (dd, $J$ = 8.2, 2.0 Hz, 1 H), 6.21 (s, 2 H), 5.83 (s, 2 H), 5.00 (s, 2 H), 3.73 (s, 3 H), 3.52 (s, 2 H). $^{13}$C NMR (126 MHz, DMSO-$d_6$): $\delta$ 162.4, 161.7 (d, $J$ = 243.4 Hz), 161.5, 154.1, 149.0, 146.0, 133.6 (d, $J$ = 2.9 Hz), 133.0, 129.9 (d, $J$ = 8.3 Hz), 120.2, 115.2 (d, $J$ = 21.3 Hz), 113.9, 112.9, 106.3, 69.3, 55.5, 32.2. $^{19}$F NMR (471 MHz, DMSO-$d_6$): $\delta$ -114.54 to -114.67 (m). HRMS(ESI+): m/z calcd for $C_{19}H_{20}FN_4O_2$ ([M+H]$^+$): 355.1565; found: 355.1572.

### *Synthesis of the protodeboronation product*

The synthesis of 5-(4-(benzyloxy)-3-methoxybenzyl) pyrimidine-2,4-diamine is schematically shown in Figure 3.

### 4-(Benzyloxy)-3-methoxybenzaldehyde: Compound 7

To obtain compound 7, 226 µl of benzyl bromide (1.9 mmol), 0.304 g of vanillin (1/998 mmol), and 0.394 g of potassium carbonate (2.85 mmol) were suspended in 18.5 ml MeCN in a 50-ml flask. Then, a condenser was used to fit the flask, and, to reflux with stirring for 180 minutes, the mixture was heated. The solvent was then removed in declined pressure, and the solids were suspended in toluene for loading on a flash column. Flash chromatography (silica, 0%-20% EtOAc/petroleum ether) was used to purify the crude product, which resulted in a pale yellow oil in a 94% yield. $^1$H NMR (500 MHz, DMSO-$d_6$): $\delta$ 9.84 (s, 1 H), 7.54 (dd, $J$ = 8.2, 1.9 Hz, 1 H), 7.50-7.43 (m, 2 H), 7.42 (d, $J$ = 1.9 Hz, 1 H), 7.44-7.38 (m, 2 H), 7.39-7.32 (m, 1 H), 7.27 (d, $J$ = 8.3 Hz, 1 H), 5.22 (s, 2 H), 3.84 (s, 3 H). $^{13}$C NMR (126 MHz, DMSO-$d_6$): $\delta$ 191.4, 153.2, 149.4, 136.3, 129.8, 128.5, 128.1, 128.0, 125.9, 112.6, 109.7, 70.0, 55.6.

### 2-(4-(Benzyloxy)-3-methoxybenzyl)-3-(phenylamino)acrylonitrile: Compound 8

The preparation of 2-(4-(benzyloxy)-3-methoxybenzyl)-3-morpholinoacrylonitrile was as follows: 0.450 g of compound 7 (1.9 mmol) and 251 µl of 4-morpholinopropionitrile (1 eq.) were dissolved in 4.5 ml DMSO in a round-bottom flask; 22 mg of NaH (60% dispersion in mineral oil, 0.3 eq.) was mixed, and the suspension was heated at 70°C for 30 minutes. The reaction solvent was quenched into brine, and the obtained suspension was extricated 2× with EtOAc. The organic phase was separated, dried over $Na_2SO_4$, and filtered; the solvent was deleted in declined pressure. Flash chromatography (silica, 0%-80% EtOAc/petroleum ether) was used to purify the crude product, which resulted in 0.579 g yellow solid in an 86% yield. The resulting compound was used immediately for the preparation of compound 9.

### 2-(4-(Benzyloxy)-3-methoxybenzyl)-3-morpholinoacrylonitrile: Compound 9

To obtain compound 9, 0.579 g of compound 8 (1.6 mmol) and 0.226 g of aniline hydrochloride (1.74 mmol) were suspended in 6 ml isopropanol. The obtained solvent was heated to reflux for half an hour and cooled at room temperature. Water (1 ml) was added dropwise, then the flask was put at −5°C for half an hour, and the precipitate was extracted using filtration. Flash chromatography (silica, 0%-50% EtOAc/petroleum ether) was applied to purify the crude product to yield 0.428 g of product as a beige solid in a 73% yield. $^1$H NMR (500 MHz, DMSO-$d_6$): $\delta$ 9.10 (d, $J$ = 12.6 Hz, 1 H), 7.62 (d, $J$ = 12.6 Hz, 1 H), 7.47-7.41 (m, 2 H), 7.42-7.35 (m, 2 H), 7.36-7.29 (m, 1 H), 7.29-7.22 (m, 2 H), 7.21-7.15 (m, 2 H), 6.98 (d, $J$ = 8.2 Hz, 1 H), 6.94-6.87 (m, 1 H), 6.90 (d, $J$ = 2.1 Hz, 1 H), 6.76 (dd, $J$ = 8.2, 2.0 Hz, 1 H), 5.05 (s, 2 H), 3.76 (s, 3 H), 3.42 (s, 2 H). $^{13}$C NMR (126 MHz, DMSO-$d_6$): $\delta$ 149.1, 146.5, 142.4, 141.8, 137.3, 132.7, 129.2, 128.4, 127.77, 127.75, 121.2, 120.1, 119.5, 115.2, 113.8, 112.5, 80.8, 70.0, 55.6, 36.0.

### 5-(4-(Benzyloxy)-3-methoxybenzyl) pyrimidine-2,4-diamine: BOMPyD

To obtain BOMPyD, 0.428 g of compound 9 (1.2 mmol) and 0.110 g of guanidine hydrochloride (1.15 mmol) were suspended in 12 ml EtOH in a 25-ml round bottom flask; 3.5 ml 0.5 M NaOMe solution (0.75 mmol) was added with stirring, and the resulted mixture was fitted with a

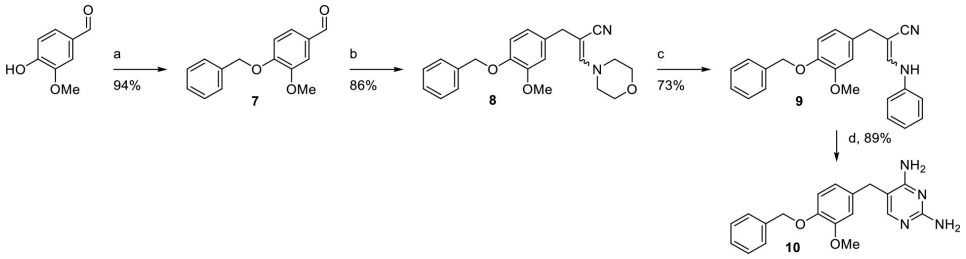


***Figure 3.*** *HPLC trace (UV in blue, radioactivity in red) of (A) [$^{18}$F]FOMPyD, (B) [$^{18}$F]FOMPyD co-injected with cold FOMPyD, and (C) protodeboronation side-product BOMPyD on a Phenomenex Prodigy ODS-3 column (250 × 4.6 mm, 10 µm), 40:60 MeCN:0.1% TFA, 0.7 ml·minute$^{-1}$, monitored at 210 nm. The solvent feature at 3.8 min is the DMSO matrix used for the standard cold injection.*

condenser and stirred at reflux for 20 hours. The solution was put at room temperature; 1.5 ml 2 M NaOH solution was mixed. Then, the mixture was put at 5°C for half an hour. The obtained precipitate was aggregated using filtration and washed with cold EtOH. Flash chromatography (silica, 0%-15% MeOH/DCM) was applied to purify the crude product and isolated as 0.303 g of pale yellow powder in an 89% yield. $^{1}$H NMR (500 MHz, DMSO-$d_6$): $\delta$ 7.46 (s, 1 H), 7.44-7.41 (m, 2 H), 7.40-7.36 (m, 2 H), 7.34-7.29 (m, 1 H), 6.92 (d, $J$ = 8.2 Hz, 1 H), 6.89 (d, $J$ = 2.0 Hz, 1 H), 6.68 (dd, $J$ = 8.2, 2.0 Hz, 1 H), 6.25 (s, 2 H), 5.88 (s, 2 H), 5.02 (s, 2 H), 3.73 (s, 3 H), 3.53 (s, 2 H). $^{13}$C NMR (126 MHz, DMSO-$d_6$): $\delta$ 162.4, 161.4, 153.8, 149.0, 146.1, 137.3, 132.8, 128.4, 127.8, 127.7, 120.2, 113.8, 112.9, 106.4, 70.0, 55.5, 32.2.

### *Radiolabeling and quality control*

Without adding carrier aqueous, [$^{18}$F] fluoride was developed using an $^{18}$O (p, n) $^{18}$F nuclear reaction on augmented [$^{18}$O] $H_2O$ in a liquid target (Nitra XL) of the cyclotron (IBA Cyclone 18/9 MeV). The drying, labeling, and purification of [$^{18}$F] fluoride were performed on a synthesis module (Scintomics GRP) that contained a preparative HPLC (Knauer) with UV and radioactivity detectors utilizing a semi-automated disposable manifold setup. [$^{18}$F] $F^-/H_2O$ (200–500 mCi) from the target was passed through an unconditioned Sep-Pak Light QMA cartridge (46 mg, Waters) from the male side. Afterward, the cartridge was flushed with anhydrous MeOH (3 ml) to find and remove traces of water. Next anhydrous [$^{18}$F] fluoride was mixed with TEAB solution in MeOH (450 µL, 1 mg/mL). Then, the obtained solvent was mixed with neat MeOH (500 µL) from the female side into a 5-mL conical Wheaton vial. Afterward, in a vacuum environment, the solvent was deleted at 100 °C, initially using a stream of argon (100 mL/min, 8 minutes) and thereafter in a closed system (2 minutes). Finally, we quenched the vacuum with air. Then, we charged the reaction vial with a freshly-prepared solution of boronate precursor 6 (8.6 mg, 10 µmol) and $Cu(OTf)_2Py_4$ (6.8 mg, 10 µmol) in a mixture of DMA (300 µL) and 1-BuOH (150 µL), and the solution could react for 10 minutes at 110 °C and then for an additional similar period at 130 °C.

The resulted crude mixed solvent was cooled and diluted with HPLC eluent (1.5 mL). Then, it was injected into the semi-preparative HPLC system (30% MeCN: 70% 20 mM $NaH_2PO_4$, 4 mL/min). Purified [$^{18}$F]FOMPyD was collected from the HPLC (rt = 22-24 minutes), diluted with 20 mL $H_2O$, and trapped in a preconditioned (5 mL EtOH, followed by 10 mL water) Sep-Pak C18 Light cartridge. The cartridge was washed with 10 mL of water to eliminate all traces of MeCN; then, the tracer was eluted with 0.5 mL EtOH, and its density was reduced using saline. The resulting dose of [$^{18}$F]FOMPyD (300-450 MBq) was used in the microPET and autoradiography procedures. The quality control of the isolated [$^{18}$F]FOMPyD was performed by applying an Agilent 1200 analytical HPLC system (Phenomenex Prodigy ODS-3, 250 × 4.6 mm, 10 µm column; 40% MeCN: 60% 0.1% TFA, 0.7 mL/min).

## Animal Study

### Autoradiography

Male Wistar rats weighing 400-500 g aged 11 months were provided from the Research Center and Experimental Animal House of TUMS for autoradiography experiments. Animals were kept in a standard condition with a 12-hour light/dark cycle with ad libitum access to water and food. The interventions were confirmed by the Animal Care Committee of TUMS. In addition, we followed the Iranian Council on Animal Care Guidelines. Human brain tissues were obtained from the brain bank of the Iran University of Medical Sciences. All subjects were sacrificed by decapitation, and the brains were rapidly detached, frozen at -80 °C, and sliced into 20-µm-thick pieces. After thawing and pre-incubation in either PBS (17 mL) or a blocking solution (100 µM, 17 mL) for 1 hour, [$^{18}$F]FOMPyD was added to bring the radioactivity concentration to 37 kBq/mL, and the slides were incubated in the tracer solution for an additional 2.5 hours. After a rinse with cold buffer (3 × 3 minutes, 0 °C), followed by cold water (1 minute, 0 °C), the marked samples were dried and put on phosphor-imaging plates with standards related to the industrial tritium activity. After 20 minutes of exposure, a plate reader (BAS 5000; Fuji or Typhoon Trio + Variable Mode Imager) was used to scan all plates.

## MicroPET

The male Wistar rats weighing 300-400 g aged 2-3 months were provided from the Research Center and Experimental Animal House of TUMS for microPET imaging experiments. All PET images were modified using a CTI Concorde R4 microPET scanner for small animals (CTI, Siemens, and Munich, Germany). All interventions were confirmed by the Animal Care Committee of TUMS (protocol code: 2017-7914). Besides, they were consistent with the Iranian Council on Animal Care Guidelines. Initially, anesthesia was applied by isoflurane at 5% with a 2-3 L/min oxygen flow, which was adjusted and maintained at 1.5%-2.5% isoflurane with a 0.8 L/min oxygen flow for the duration of the scan. The rats' brains were located at the middle of the field of view (FOV), and the 90-minute dynamic scan was performed in 32 frames (8 × 30 seconds, 6 × 60 seconds, 5 × 120 seconds, and 13 × 300 seconds) concomitantly with the bolus injection of [$^{18}$F] FOMPyD in a tail vein. The average activity of injected tracer was 17.5 MBq, and the average injected volume was 0.7 mL. A 9-minute transmission scan preceded each emission scan with a 57Co point source to correct for the attenuation.

## Image Analysis

We reconstructed all images using Maximum A Posteriori (MAP) algorithm. In addition, all images were modified for scattering, dead time, and perish. Processing and analysis of images were performed by MINC tools. Eyes, nose bones, and skull base were applied as markers to co-document the PET-to-MRI images. Delineation of the region of interest (ROI) was due to the Waxholm Space atlas of the rat brain. Radioactivity counts were normalized to the weight of animals, and the injected radioactivity was expressed in Standardized Uptake Value (SUV) due to the following equation:

$$SUV = \frac{Radioactivity\,Counts * Body\,Weight\left(g\right)}{Injected\ Dose\left(Bq\right)}$$

The trapezoidal approach was applied to compute the area under the curve (AUC) of time-activity curves (TAC).

## Statistical Analysis

A two2-tailed paired *t*-test was performed using SPSS to identify the difference in [$^{18}$F]FOMPyD binding between baselines and blocking experiments, measured with PET imaging technique. Considering in vitro autoradiography data, a 2-sided unpaired *t* test was performed to identify the significance of various blocking agents-induced variations in [$^{18}$F]FOMPyD binding in rat and human brain tissues.

## Results

Due to different analyses, the BOC (tert-butyloxycarbonyl) protecting group, chemically a $Boc_2O$, is regarded to be the most probable and popular amine-protecting group in nonpeptide chemistry. On the other hand, the reaction situations to protect amine have suitable flexibility, and the method usually results in a high yield and quick conversion under relatively mild conditions. In general, it is run in water/THF, water, MeCN, or THF in the existence of a base under moderate heat (40 °C) or at room temperature.

Furthermore, the study indicated that MeOH and dioxane work as solvents for the reaction, whereas reflux of a biphasic mixture of water and chloroform with sodium bicarbonate is regarded as one the most effective and widely used methods. Thus, the usual transformation bases include DMAP, sodium bicarbonate, and sodium hydroxide. On the other hand, deprotecting a Boc-protected amine was proposed as convenient carbamate hydrolysis under acidic situations. Hence, starting material's dissolution was observed in an organic solvent such as DCM, EtOAc, toluene, or water. The concentrated hydrochloric acid or TFA the reaction is rapid run and occurs at room temperature. Therefore, it is possible to utilize the biphasic systems with a protected amine, which was dissolved in the natural phase blended with an aqueous solvent of an acid.

Two other popular deprotection techniques avoid applying strong acid, and, consequently, they may be profitable for acid-labile compounds. On the other hand, the trade-off was introduced as one of the relatively more complicated reaction setups, and it prolongs the reaction duration from 2 to 3 days. Thus, the 2 applied reagents involve zinc bromide and trimethylsilyl iodide (TMSI), and dissolution of starting substance is seen in an organic solvent such as DCM accompanied by a reagent (TMSI is generally mixed gradually). Thus the reaction continues by shaking at room temperature for 12 to 24 hours. Based on the results of a study of the reactions of amines copper-mediated [$^{18}$F]fluorination, these reactions need an acid-catalyzed Boc-deprotection, and their acid is usually concentrated HI or HCl at a temperature of 130 °C. Therefore, this catalysis is not proper for several acid-sensitive (even those with less sensitivity) compounds. The purpose is to use thermal fission of 4 Boc-protecting families to inhibit acid-catalyzed de-carboxylation. Thus, a novel synthesis approach is needed to delete the acidic deprotection of bis-Boc $^{18}$F-labeled intermediary (synthesis through conventional SNAr [$^{18}$F]fluorination such as [$^{18}$F]T807 and [$^{18}$F]MK-6240). It decreased the number of operations needed to synthesize, as well as the losses that occur in the course of deprotecting and neutralizing the obtained mixture before purification of HPLC. Furthermore, the synthesis process is automatically done with a single-use cassette on an IBA Synthera+ synthesis module that prepares the radioligand with a reliable radiochemical yield (RCY), high radiochemical purity (RCP), and increased molar activity.

## Discussion

Researchers have generally used [$^{18}$F]MK-6240 synthesized with the mentioned method (n > 60) in human and animal PET imaging investigations [17]. Thus, the coordinated copper-mediated [$^{18}$F]fluorination of the boronic acid esters with tert-butyloxycarbonyl protecting group's deprotection has not yet been investigated by the best scientific approach. This problem was proved by the step-by-step heating approach (110 °C → 130 °C) as reported earlier. The 2.6-13.1 GBq of [$^{18}$F] $F^-$ was provided, and then the [$^{18}$F]FOMPyD complex was provided with an RCY of 8.7 ± 2.8%, molar activity (Am) = 187000±93000 MBq/μmol, and RCP greater than 99% ($n$ = 4). One of the most important findings of this study is that the [$^{18}$F] FOMPyD complex is free of unreacted compound **6** and other non-radioactive impurities, involving BOMPyD, as a side-product of the chemical bond cleavage reaction by acids, which is the main and most well-known side-product in this reaction [18]. This approach indicates an important advancement following the 4 previously reported steps, and, for the first time, it makes it possible to assess the [$^{18}$F]FOMPyD complex by autoradiography in the dead brain tissues of humans and rats (in vitro), as well as PET imaging in wild rats (in vivo).

At the onset of in vitro autoradiography experimentations on the rats' brain tissues, the [$^{18}$F]FOMPyD complex was fully bonded to almost all regions. This obstruction, which is almost the same in all the areas, is a common characteristic of moderate binding because the signal in all analyzed areas ($P$ < 0.05), especially in all the areas of the cerebral cortex (Δ=37.4%, $P$ < 0.001) (Figure 4), could be blocked by non-radioactive FOMPyD (100 μM).

To study the binding selectivity deeper, heterologous occlusion examinations were done on the rats and brain samples of the human against a group of kinase inhibitors. These inhibitors involve the side-generation of protodeboronation (BOMPyD), [$^{11}$C]-(R)-3 ([$^{11}$C]-(R)-IPMICF16), which is a first-in-class PET TrkB/C-targeting radiolabeled kinase inhibitor (TrkB/C $IC_{50}$ = 0.57/0.37 nM, respectively) [19]. It is one of the most potent and peripherally selective limited Pan-Trk inhibitors (PF-06273340) (TrkA/B/C $IC_{50}$ = 6/4/3 nM, respectively) [20] and 4-[2((1R,2R)-2-hydroxycyclohexylamino)-benzothiazol-6-yloxyl]-pyridine-2-carboxylic acid methylamide (BLZ945) that is one of the small molecule inhibitors of the CSF1R kinase activities [21]. The BOMPyD (as a by-product of the protodeboronation reaction), which is an analog of the GW2580 compound and inhibits both CSF1 receptors and Trk, blocks almost all of these receptors throughout the rats' cortex region with a maximum affinity (Δ = 42.1 ± 6.8%; $t$ [28] = 10.574, $p$ < 0.001, $n$ = 15).

PF-06273340, which is a selective suppressor of Trk, indicated a considerable occlusion (Δ = 13.2 ± 9.7%; $t$ [28] = 2.460, $p$ < 0.05, $n$ = 15), whereas (R)-IPMICF22, which is another inhibitor in this category, decreased the ability of the [$^{18}$F]FOMPyD complex for binding, and thus its efficiency is significantly lower (Δ = 10.9 ± 15.9%, $t$ [28] = 1.948, $p$ = 0.06, $n$ = 15). BLZ945 (Δ = -0.1 ± 8.6%, $t$ [28] = 0.010, $p$ = 0.99, $n$ = 15) has no important impact on the declined binding of the [$^{18}$F]FOMPyD complex. BOMPyD is the most efficient blocking agent in rats' cortex and the posterior cingulate cortex regions of human brain tissue (Δ = 41.1 ± 17.3%, $t$ [6] = 3.170, $p$ < 0.05, $n$ =

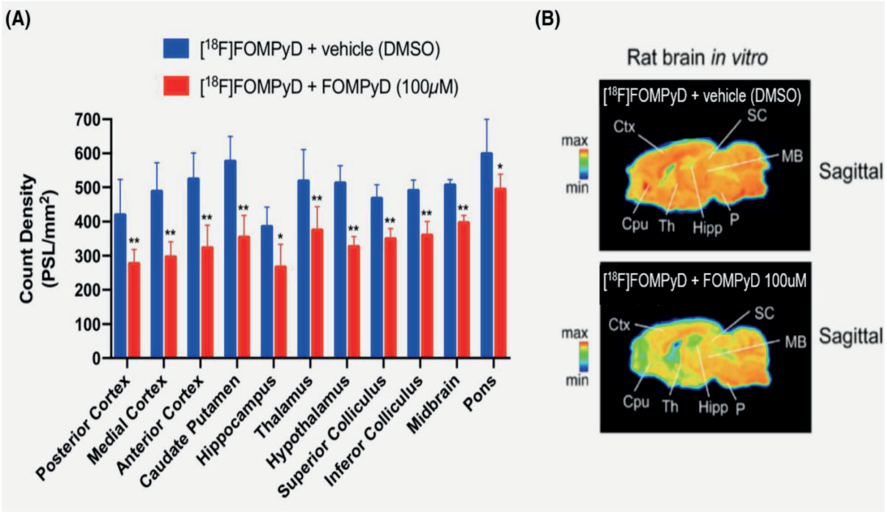


***Figure 4.*** *In vitro description of [$^{18}$F]FOMPyD over the brain sections of the rats: incubation of the sagittal samples (20 μm) with 5-(4-((4-[18F] fluorobenzyl) oxy)-3-methoxybenzyl) pyrimidine-2, 4-diamine and dimethylsulfoxide. (A). Regional quantification for in the glass autoradiography of 5-(4-((4-[18F] fluorobenzyl) oxy)-3-methoxybenzyl) pyrimidine-2, 4-diamine in the normal rats' brains. (B). Indicative in-glass autoradiography of 5-(4-((4-[18F] fluorobenzyl) oxy)-3-methoxybenzyl) pyrimidine-2, 4-diamine in the rats' brains. The base-line and 5-(4-((4-[18F] fluorobenzyl) oxy)-3-methoxybenzyl) pyrimidine-2, 4-diamine self-obstructing were compared. Moreover, * and ** respectively imply the p < 0.05 and p< 0.001.*

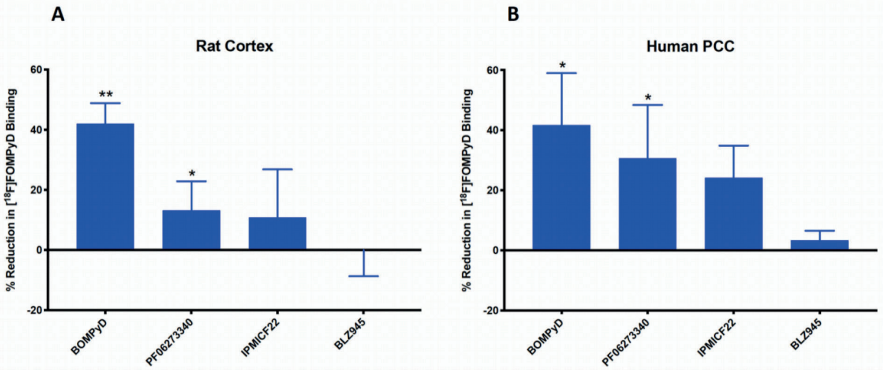


***Figure 5.*** *Description of [18F]FOMPyD binding blockage applying the in-vitro autoradiography with 4 distinct Trk or CSF-1R suppressors (100 µM). (A). The rats' cortical regions in 20 µm slices, (B). The humans' posterior cingulate cortex (PCC, 20 µm slices). Moreover, * and ** respectively show the p < 0.05 and p< 0.001. Figures S4 and S5 indicate the source images, and fig. S6 shows the chemical compounds of inhibitors.*

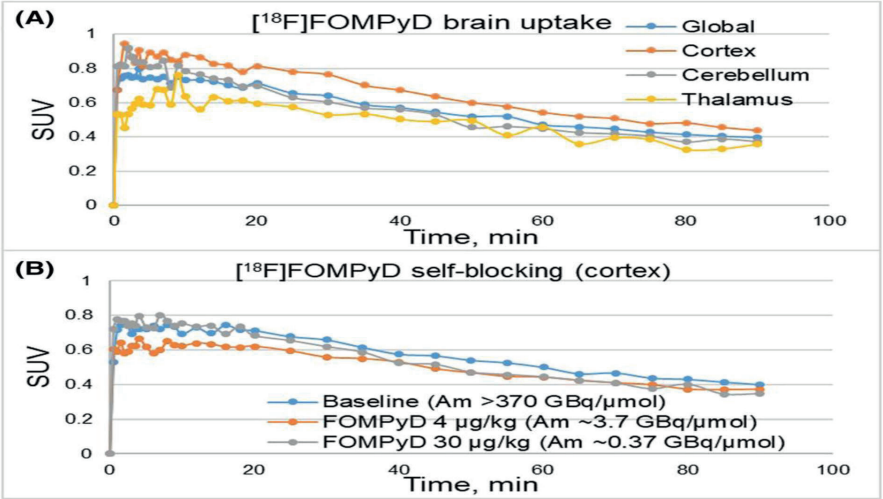


***Figure 6.*** *Time-activity graphs of 5-(4-((4-[18F] fluorobenzyl) oxy)-3-methoxybenzyl) pyrimidine-2, 4-diamine in the Wistar rats' brains. (A). The regional dispersion at the base-line imaging (n= 2, Figure S7 indicates the source image). (B). self- obstructing by 5-(4-((4-[18F] fluorobenzyl) oxy)-3-methoxybenzyl) pyrimidine-2, 4-diamine resulted in a smaller uptake decline in the cortical regions (ΔAUC40–90 = 11.1±0.7%; t (2) = 74.01, p < 0.001; n = 3) at certain dose concentrations ranging between 0/004 and 0/03 mg/kg (obstructing information has been presented in one of the rats).*

4), while the efficiency and effectiveness of PF-06273340 ($\Delta = 30.6 \pm 17.8\%$, $t$ [6] = 2.529, $p < 0.05$, $n$ =4) are higher in the human cortical tissues compared to the rat brain tissue (Figure 5). As mentioned in Figure 5, blockage by IPMICF22 ($\Delta = 24.2 \pm 10.7\%$, $t$ [6] = 1.958, $p = 0.098$, $n$ = 4) efficiently decreases [$^{18}$F]FOMPyD binding; nevertheless, this obstruction is not statistically significant. At last, BLZ945 ($\Delta = 3.2 \pm 3.3\%$, $t$ [6] = 0.332, $p = 0.75$, $n = 4$), as another CSF-1 or TKI, did not decrease [$^{18}$F]FOMPyD binding, which is consistent with the data from the rat cortex (Figure 5).

Due to in vitro data, the function of the inhibitors that affect the binding of [$^{18}$F]FOMPyD complex is as follows:

Kinase inhibitors, such as FOMPyD and BOMPyD, whose bases and chemical structures are due to GW2580 chemical structure, have indicated the highest efficiency and effectiveness in decreasing the binding to the [$^{18}$F] FOMPyD complex. The blocking efficiency of type I TKI (IPMICF22) was statistically less and lower due to quantity and quality, respectively. Therefore, the CSF-1 receptor inhibitor (BLZ945) had almost no significant impact on the binding of the [$^{18}$F]FOMPyD complex, neither in the cortex of wild-type rats nor in the human brain tissues. The first microPET scans of the research indicated just medium absorbent of the [$^{18}$F]FOMPyD complex in the wild rats (totality brain SUVmax = 0.71 ± 0.04, $n$ = 2) with the most persistence in the cortex (Figure 6).

## Conclusion

The preparation of 5-(4-((4-[$^{18}$F] fluorobenzyl) oxy)-3-methoxybenzyl)pyrimidine-2,4-diamine is indicated for PET imaging of the TrkB/C receptor. Thus, as a potential theory, this combination can be applied to identify degenerative diseases and subsequently prevent

shortage of [18F]FOMPyD due to many reasons, such as high cost and different difficulties in production, this compound can be applied as a PET detector for CNS imaging. Thus, poor pharmacokinetic features of 5-(4-((4-[18F] fluorobenzyl)oxy)-3-methoxybenzyl)pyrimidine-2,4-diamine prevented its utilization as a PET radioligand in brain scanning likely, but 1-pot synthesis is a strategy to improve the effectiveness of the chemical reaction that occurs by the use of copper, 18F-fluorination, and Boc-deprotection, is an approach for the radio-synthesis of PET tracers which are sensitive to acid.

## Acknowledgements
This approach is part of the PhD thesis of Seyyed Hossein Hassanpour, and we would like to express our special thanks to TUMS and AEOI for their financial support.

## Availability of Data and Material
Data supporting the findings of this approach are available in the supplementary section.

## Authors' contributions
All laboratory work and writing of the article were done by SH Hassanpour. The initial editing of the manuscript was done by Dr Alireza Doroudi and the final editing of the article was done by SZ Karami.

## Conflict of interests
The authors declare that there is no conflict of interest regarding the publication of this article.

## Consent to participate
This research includes does not any studies with human participants. All interventions have been confirmed by the Animal Care Committee of Tehran University of Medical Sciences (protocol # 2017-7914). Besides, they were consistent with the Iranian Council on Animal Care Guidelines.

## Ethical Approval
All interventions have been confirmed by the Animal Care Committee of Tehran University of Medical Sciences (protocol # 2017-7914).

## Funding
Tehran University of Medical Sciences, Grant/Award Numbers: MPRC-9715, MPRC-9715.

## Author details
Seyyed Hossein Hassanpour[1], Alireza Doroudi[2], Seyyedeh Zeinab Karami[3]

1. Young Researchers and Elite Club, Yassoj Branch, Islamic Azad University, Yasooj, Iran
2. Department of Medicinal Chemistry, School of Pharmacy, Ahvaz Jundishapur University of Medical Sciences, Ahvaz, Iran
3. Department of Biology, Faculty of Basic Sciences, Yasouj University, Yasouj, Iran

## References
1. Huang EJ, Reichardt LF. Trk Receptors: Roles in Neuronal Signal Transduction. Annu Rev Biochem.2003;72(1):609-42. https://doi.org/10.1146/annurev.biochem.72.121801.161629
2. Massa SM, Yang T, Xie Y, Shi J, Bilgen M, Joyce JN, et al. Small molecule BDNF mimetics activate TrkB signaling and prevent neuronal degeneration in rodents. J Clin Invest. 2010;120(5):1774-85. https://doi.org/10.1172/JCI41356
3. Stoilov P, Castren E, Stamm S. Analysis of the human TrkB gene genomic organization reveals novel TrkB isoforms, unusual gene length, and splicing mechanism. Biochem Biophys Res Commun. 2002;290(3):1054-65. https://doi.org/10.1006/bbrc.2001.6301
4. Yeo GS, Connie Hung CC, Rochford J, Keogh J, Gray J, Sivaramakrishnan S, et al. A de novo mutation affecting human TrkB associated with severe obesity and developmental delay. Nat Neurosci. 2004;7(11):1187-9. https://doi.org/10.1038/nn1336
5. Gupta V, You Y, Gupta V, Klistorner A, Graham S. TrkB Receptor Signalling: Implications in Neurodegenerative, Psychiatric and Proliferative Disorders. Int J Mol Sci.2013;14(5):10122-42. https://doi.org/10.3390/ijms140510122
6. Galland F, Stefanova M, Lafage M, Birnbaum D. Localization of the 5' end of the MCF2 oncogene to human chromosome 15q15→q23. Cytogenet Cell Genet. 1992;60 (2):114-6. https://doi.org/10.1159/000133316
7. Xu Q, Malecka KL, Fink L, Jordan EJ, Duffy E, Kolander S, et al. Identifying three-dimensional structures of autophosphorylation complexes in crystals of protein kinases. Science Signaling. 2015;8(405):rs13. https://doi.org/10.1126/scisignal.aaa6711
8. Meyers MJ, Pelc M, Kamtekar S, Day J, Poda GI, Hall MK, et al. Structure-based drug design enables conversion of a DFG-in binding CSF-1R kinase inhibitor to a DFG-out binding mode. Bioorg Med Chem Lett. 2010;20(5):1543-7. https://doi.org/10.1016/j.bmcl.2010.01.078
9. Mitrasinovic OM, Grattan A, Robinson CC, Lapustea NB, Poon C, Ryan H, et al. Microglia overexpressing the macrophage colony-stimulating factor receptor are neuroprotective in a microglial-hippocampal organotypic coculture system. J Neurosci. 2005;25(17):4442-51. https://doi.org/10.1523/JNEUROSCI.0514-05.2005
10. Li M, Li Z, Ren H, Jin WN, Wood K, Liu Q, et al. Colony stimulating factor 1 receptor inhibition eliminates microglia and attenuates brain injury after intracerebral hemorrhage. J Cereb Blood Flow Metab.2017;37(7):2383-95. https://doi.org/10.1177/0271678X16666551
11. Narayanaswami V, Dahl K, Bernard-Gauthier V, Josephson L, Cumming P, Vasdev N. Emerging PET Radiotracers and Targets for Imaging of Neuroinflammation in Neurodegenerative Diseases: Outlook Beyond TSPO. Mol Imaging. 2018;17:1536012118792317. https://doi.org/10.1177/1536012118792317
12. Horti AG, Naik R, Foss CA, Minn I, Misheneva V, Du Y, et al. PET imaging of microglia by targeting macrophage colony-stimulating factor 1 receptor (CSF1R). Proc Natl Acad Sci. 2019;116(5):1686-91. https://doi.org/10.1073/pnas.1812155116
13. Tanzey SS, Shao X, Stauff J, Arteaga J, Sherman P, Scott PJH, et al. Synthesis and Initial In Vivo Evaluation of 11C-AZ683-A Novel PET Radiotracer for Colony Stimulating Factor 1 Receptor (CSF1R). Pharmaceuticals. 2018;11(4):136 https://doi.org/10.3390/ph11040136
14. Bernard-Gauthier V, Schirrmacher R. 5-(4-((4-[18F] fluorobenzyl) oxy)-3-methoxybenzyl) pyrimidine-2, 4-diamine: A selective dual inhibitor for potential PET imaging of Trk/CSF-1R. Bioorganic Med Chem Lett. 2014;24(20):4784-90. https://doi.org/10.1016/j.bmcl.2014.09.014

15. Tredwell M, Preshlock SM, Taylor NJ, Gruber S, Huiban M, Passchier J, et al. A General Copper-Mediated Nucleophilic 18F Fluorination of Arenes. Angew Chemie Int Ed. 2014;53(30):7751–5. https://doi.org/10.1002/anie.201404436
16. Zischler J, Kolks N, Modemann D, Neumaier B, Zlatopolskiy BD. Alcohol-Enhanced Cu-Mediated Radiofluorination. Chem - A Eur J. 2017;23(14):3251–6. https://doi.org/10.1002/chem.201604633
17. Hopewell R, Ross K, Kostikov A, Pascoal TA, Alberti T, Lacatus-Samoila M, et al. A simplified radiosynthesis of [18F] MK-6240 for tau PET imaging. J Label Compd Radiopharm. 2019;62(2):109–14. https://doi.org/10.1002/jlcr.3695
18. Mossine AV, Brooks AF, Bernard-Gauthier V, Bailey JJ, Ichiishi N, Schirrmacher R, et al. Automated synthesis of PET radiotracers by copper-mediated 18F-fluorination of organoborons: Importance of the order of addition and competing protodeborylation. J Label Compd Radiopharm. 2018;61(3):228–36. https://doi.org/10.1002/jlcr.3583
19. Bernard-Gauthier V, Bailey JJ, Mossine AV, Lindner S, Vomacka L, Aliaga A, et al. A Kinome-Wide Selective Radiolabeled TrkB/C Inhibitor for in Vitro and in Vivo Neuroimaging: Synthesis, Preclinical Evaluation, and First-in-Human. J Med Chem. 2017;60(16):6897–910. https://doi.org/10.1021/acs.jmedchem.7b00396
20. Skerratt SE, Andrews M, Bagal SK, Bilsland J, Brown D, Bungay PJ, et al. The Discovery of a Potent, Selective, and Peripherally Restricted Pan-Trk Inhibitor (PF-06273340) for the Treatment of Pain. J Med Chem. 2016;59(22):10084–99. https://doi.org/10.1021/acs.jmedchem.6b00850
21. Krauser JA, Jin Y, Walles M, Pfaar U, Sutton J, Wiesmann M, et al. Phenotypic and metabolic investigation of a CSF-1R kinase receptor inhibitor (BLZ945) and its pharmacologically active metabolite. Xenobiotica. 2015;45(2):107–23. https://doi.org/10.3109/00498254.2014.945988

## NMR and HRMS data

## Compound 1 HRMS

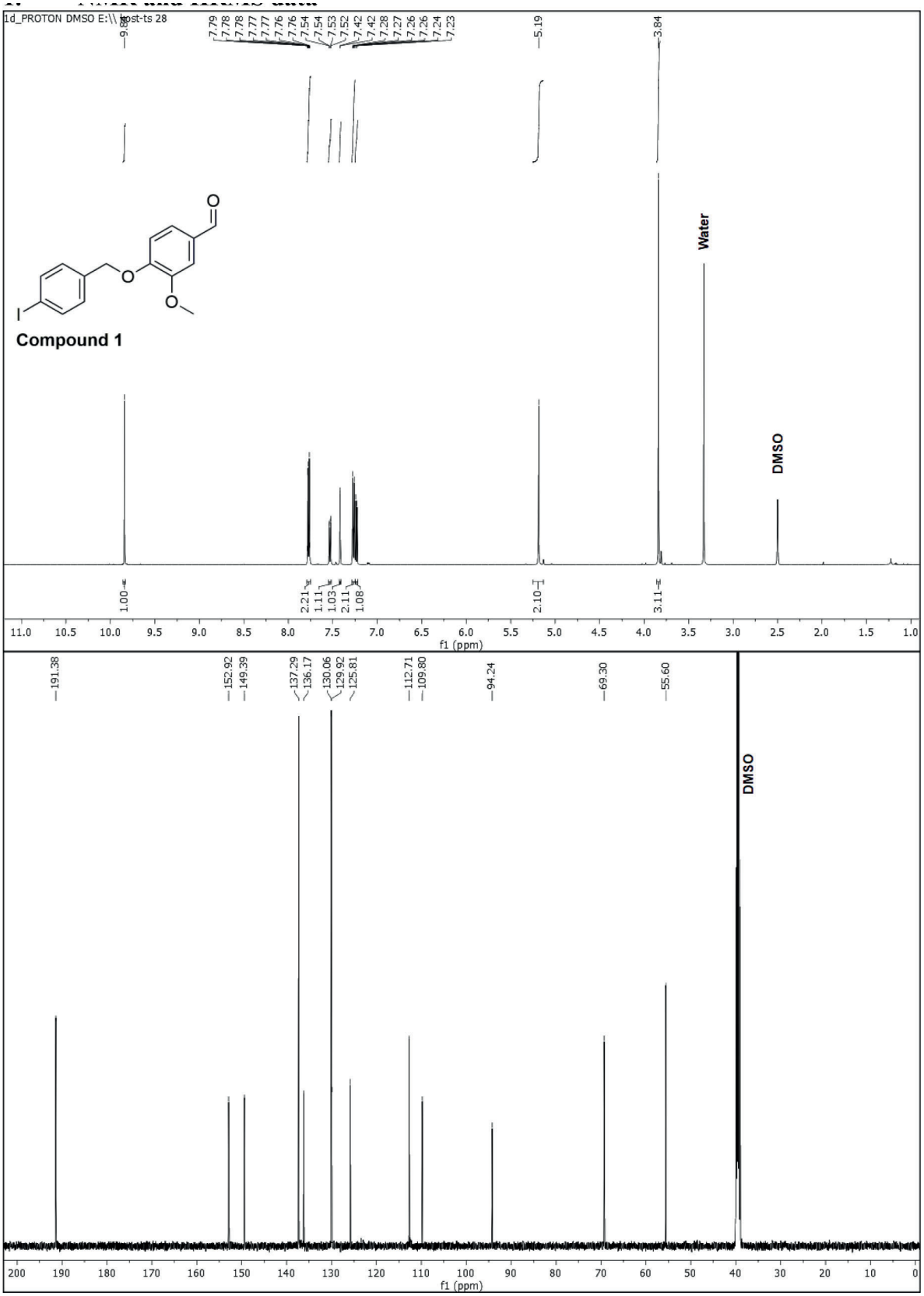

## Compound 2 HRMS

Hassanpour... 02/21/19 08:15:34

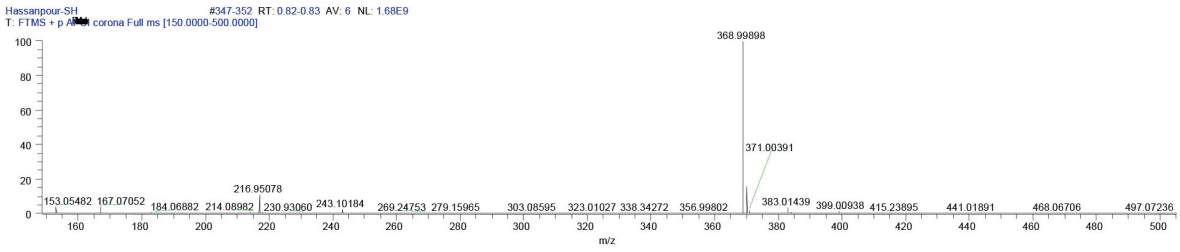


Hassanpour-SH #347-352 RT: 0.82-0.83 AV: 6
T: FTMS + p APCI corona Full ms [150.0000-500.0000]
m/z= 368.98606-369.01053

| m/z | Intensity | Relative | Resolution | Charge | Theo. Mass | Delta (ppm) | RDB equiv. | Composition |
|---|---|---|---|---|---|---|---|---|
| 368.99898 | 1681457920.0 | 100.00 | 29211.32 | 1.00 | 368.99821 | 2.07 | 8.5 | $C_{15}H_{14}O_3I$ |

Hassanpour- #347-352 RT: 0.82-0.83 AV: 6
T: FTMS + p APCI corona Full ms [150.0000-500.0000]
m/z= 216.94215-216.95809

| m/z | Intensity | Relative | Resolution | Charge | Theo. Mass | Delta (ppm) | RDB equiv. | Composition |
|---|---|---|---|---|---|---|---|---|
| 216.95078 | 190143104.0 | 100.00 | 35497.21 | 1.00 | 216.95087 | -0.42 | 4.5 | $C_7H_6I$ |

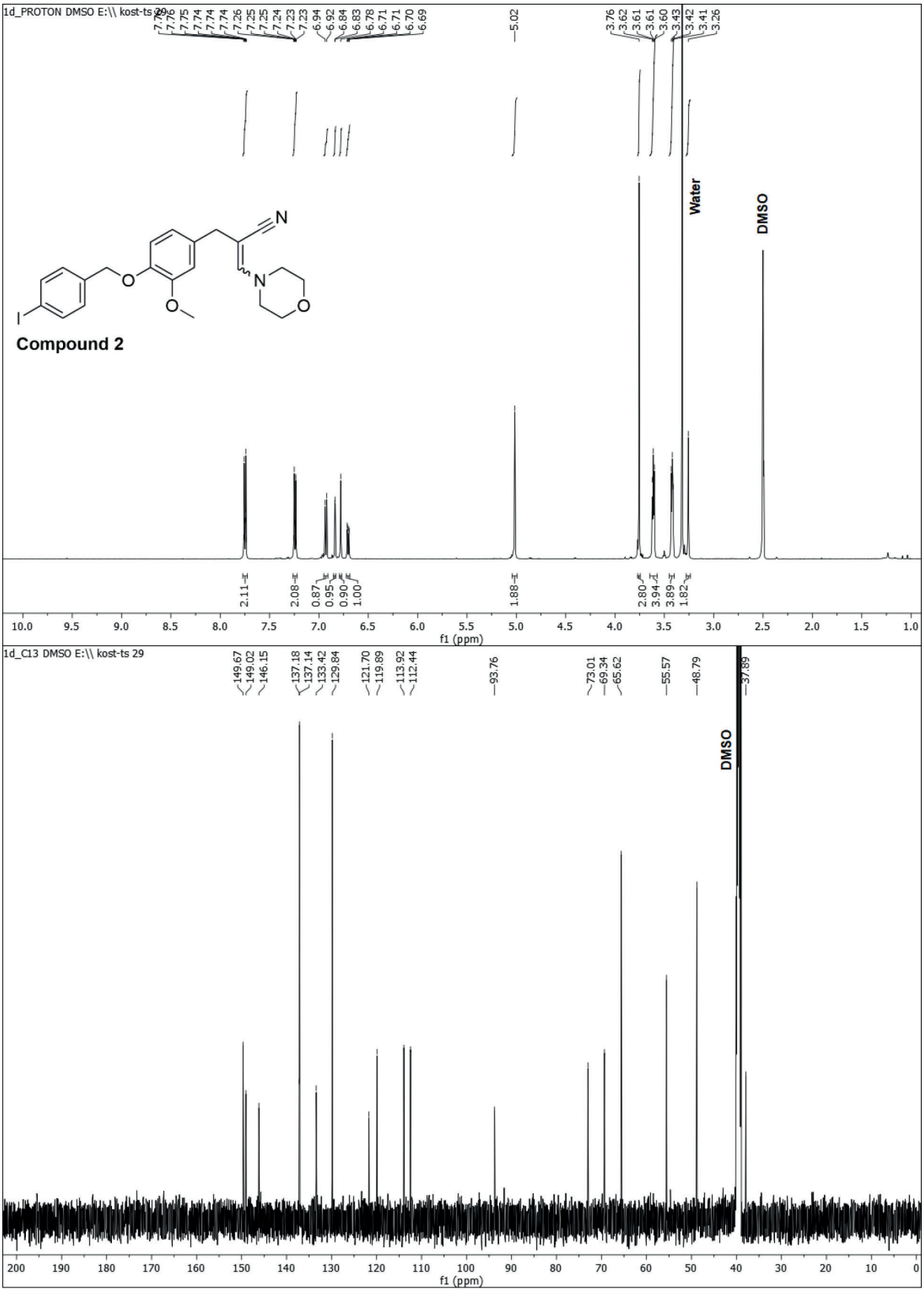
1d_PROTON DMSO E:\\ kost-ts 29
Water
DMSO
Compound 2
f1 (ppm)
1d_C13 DMSO E:\\ kost-ts 29
DMSO
f1 (ppm)

## Compound 3 HRMS

Hassanpour-SH... 02/20/19 16:20:05

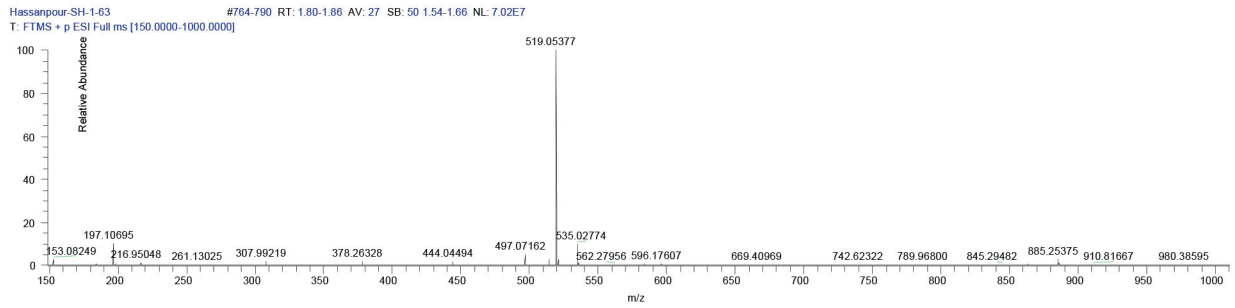


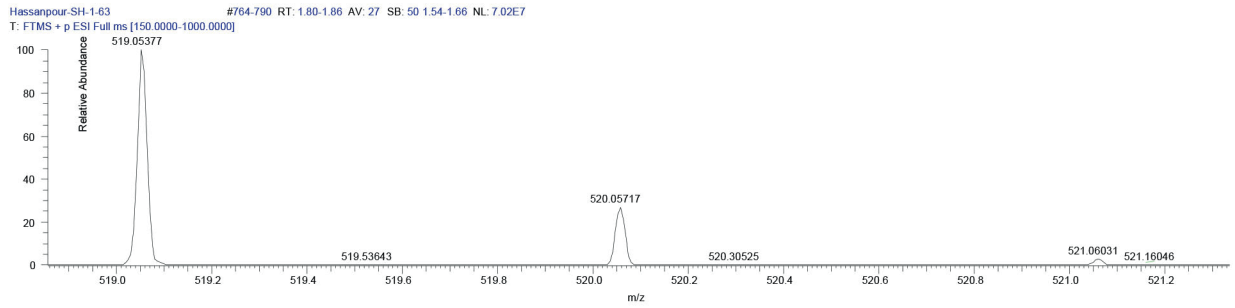


Hassanpour-SH-1-63 # RT:1.80-1.86 AV:27
SB:501.54-1.66
T:FTMS + p ESI Full ms [150.0000-1000.0000]
m/z= 519.03073-519.08074

| m/z | Intensity | Relative | Resolution | Charge | Theo. Mass | Delta (ppm) | RDB equiv. | Composition |
|---|---|---|---|---|---|---|---|---|
| 519.05377 | 70660392.0 | 100.00 | 23084.81 | 1.00 | 519.05399 | -0.42 | 14.5 | $C_{24}H_{21}O_2N_2INa$ |

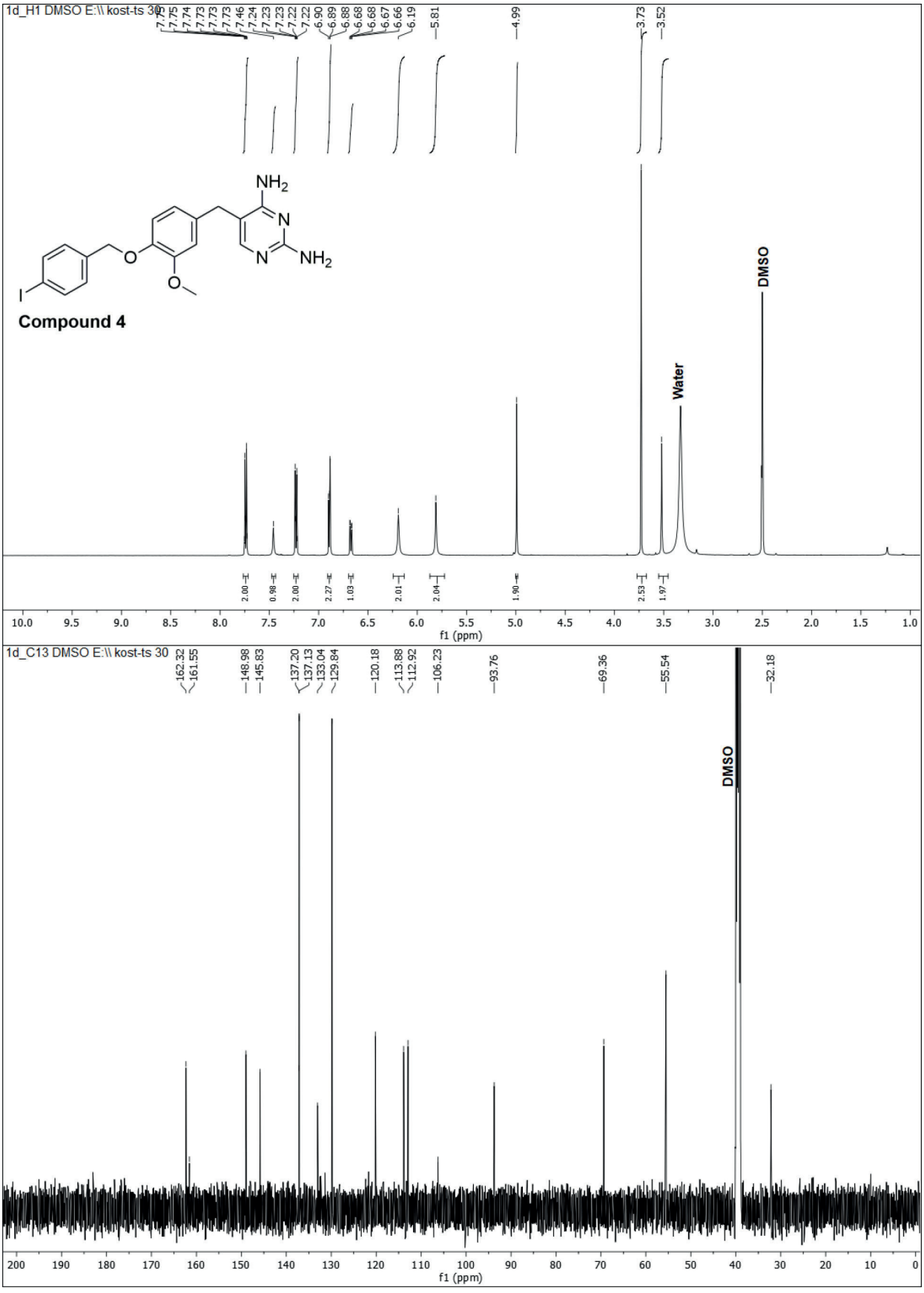
1d_H1 DMSO E:\\ kost-ts 30
7.75
7.75
7.74
7.73
7.73
7.73
7.46
7.24
7.23
7.23
7.22
7.22
6.90
6.89
6.88
6.68
6.68
6.67
6.66
6.19
5.81
4.99
3.73
3.52
NH2
N
N
NH2
O
O
I
Compound 4
DMSO
Water
2.00
0.98
2.00
2.27
1.03
2.01
2.04
1.90
2.53
1.97
10.0
9.5
9.0
8.5
8.0
7.5
7.0
6.5
6.0
5.5
5.0
4.5
4.0
3.5
3.0
2.5
2.0
1.5
1.0
f1 (ppm)
1d_C13 DMSO E:\\ kost-ts 30
162.32
161.55
148.98
145.83
137.20
137.13
133.04
129.84
120.18
113.88
112.92
106.23
93.76
69.36
55.54
DMSO
32.18
200
190
180
170
160
150
140
130
120
110
100
90
80
70
60
50
40
30
20
10
0
f1 (ppm)

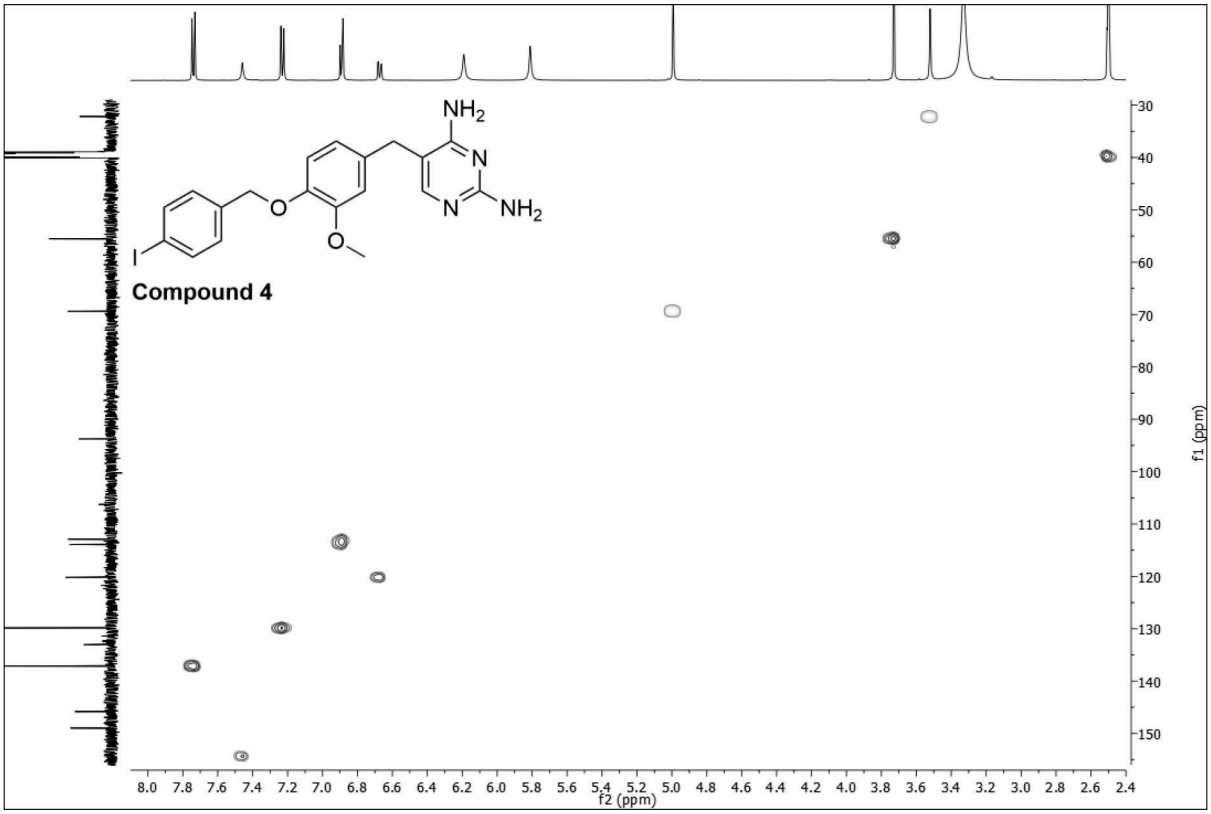


Hassanpour-SH.....-... 02/20/19 15:55:51

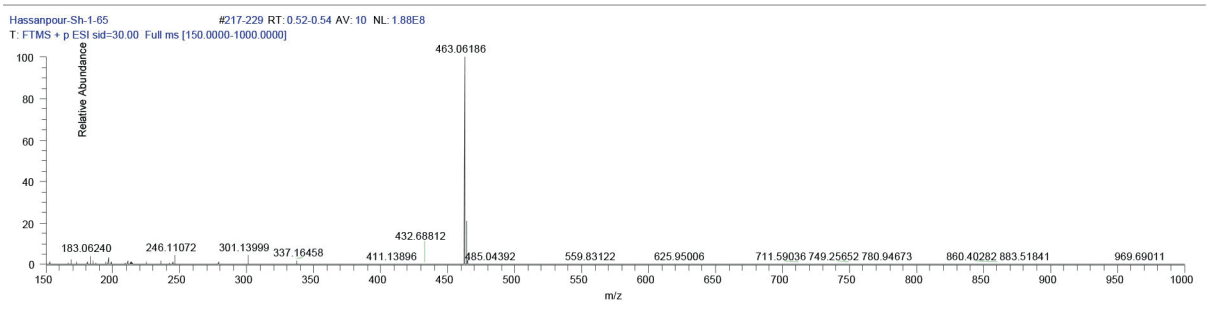


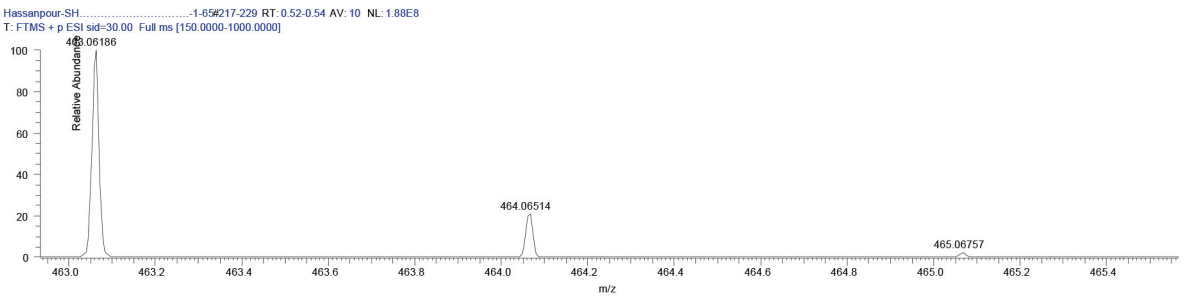


190220-02 Hssanpour-Sh- 1-65 #217-226 RT:0.52-0.54 AV:10
T:FTMS + p ESI sid=30.00 Full ms [150.0000-1000.0000]
m/z= 463.03684-463.07718

| m/z | Intensity | Relative | Resolution | Charge | Theo. Mass | Delta (ppm) | RDB equiv. | Composition |
|---|---|---|---|---|---|---|---|---|
| 463.06186 | 191402432.0 | 100.00 | 25300.72 | 1.00 | 463.06255 | -1.49 | 11.5 | $C_{19}H_{20}O_2N_4I$ |
| | | | | | 463.06389 | -4.39 | 11.0 | $C_{21}H_{22}O_3NI$ |

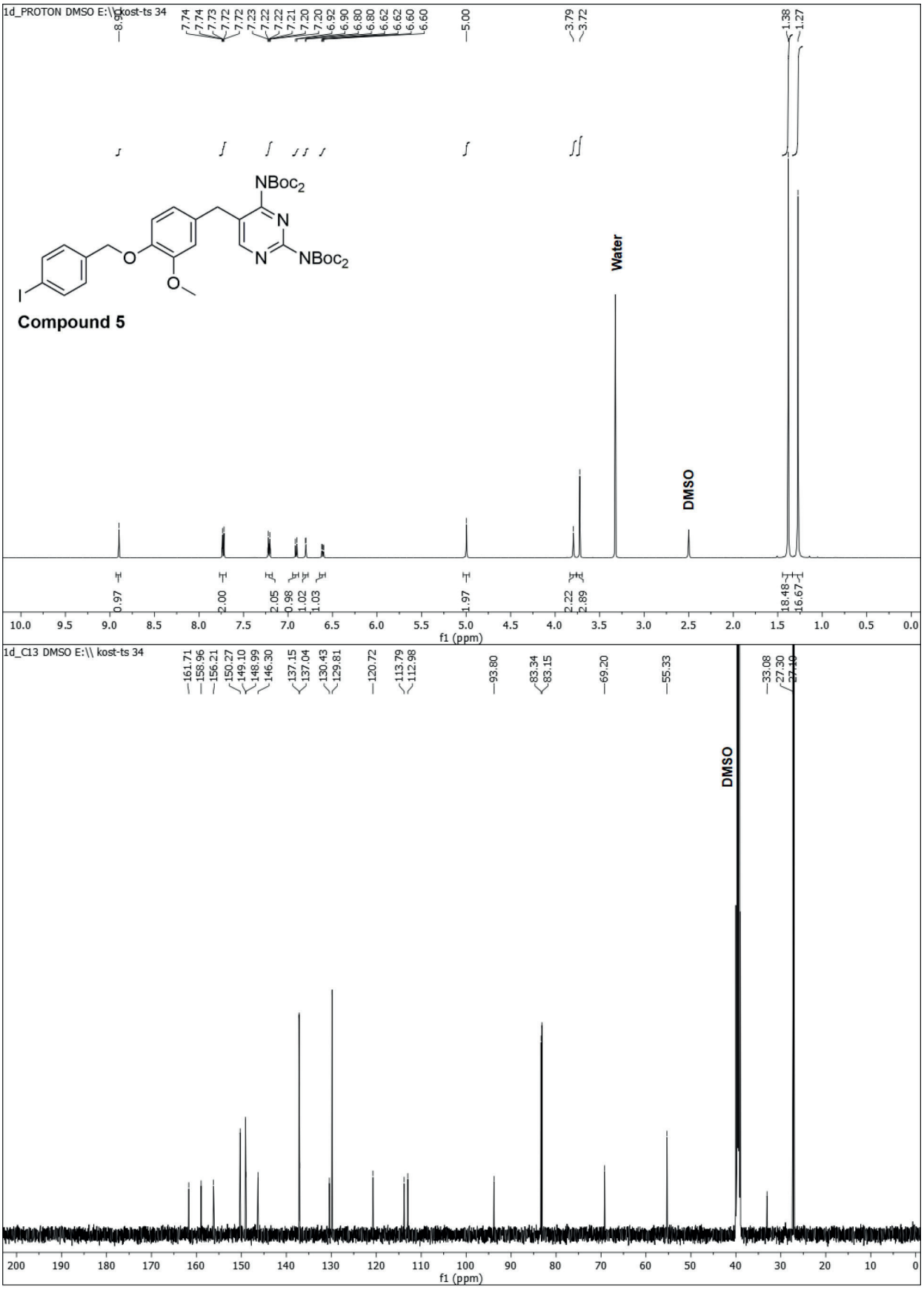
1d_PROTON DMSO E:\\ kost-ts 34
NBoc2
N
N
NBoc2
O
O
I
Compound 5
Water
DMSO
f1 (ppm)
1d_C13 DMSO E:\\ kost-ts 34
DMSO
f1 (ppm)

190220-Hassanpour-SH.....-... 02/20/19 16:13:51

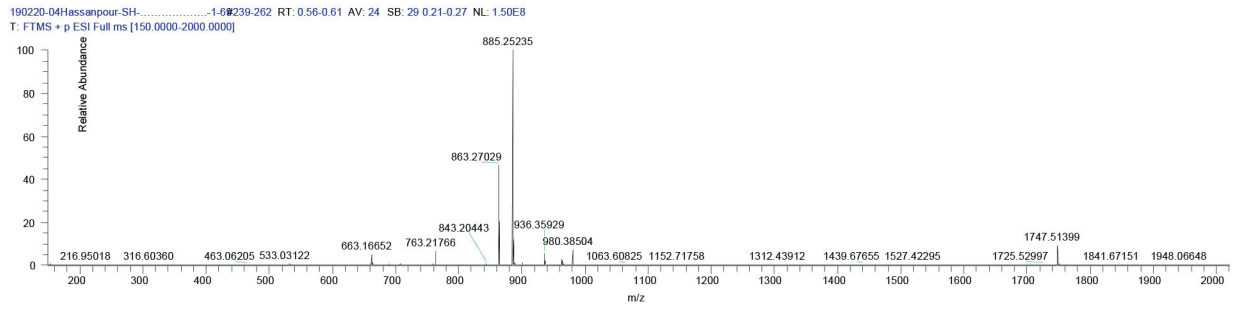


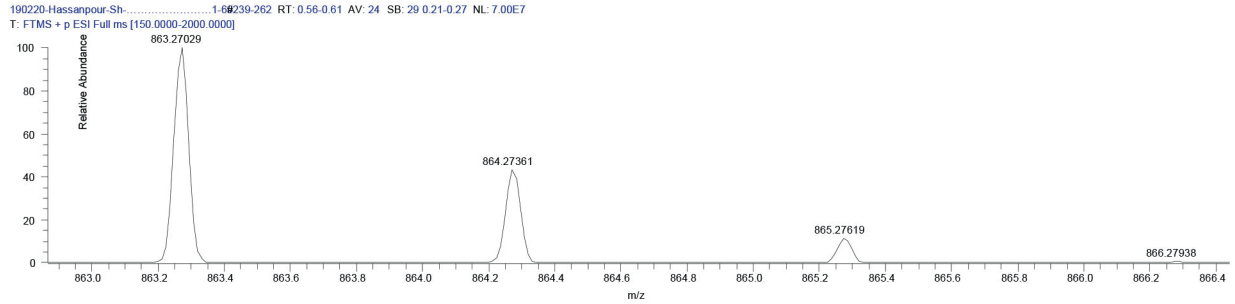


190220-Hassanpour-SH-1-69 #239-262 RT: 0.56-0.61 AV: 24
SB: 29 0.21-0.27
T: FTMS + p ESI Full ms [150.0000-2000.0000]
m/z= 863.22267-863.31779

| m/z | Intensity | Relative | Resolution | Charge | Theo. Mass | Delta (ppm) | RDB equiv. | Composition |
|---|---|---|---|---|---|---|---|---|
| 863.27029 | 70264664.0 | 100.00 | 17445.06 | 1.00 | 863.27226 | -2.29 | 15.5 | $C_{39}H_{52}O_{10}N_4I$ |
| | | | | | 863.27361 | -3.85 | 15.0 | $C_{41}H_{54}O_{11}NI$ |


1d_PROTON DMSO E:\\ kost-ts 37
8.99
7.67
7.67
7.66
7.65
7.41
7.41
7.40
7.40
6.91
6.89
6.81
6.80
6.61
6.61
6.59
6.59
5.07
3.79
3.73
1.38
1.38
1.28
1.27
NBoc2
N
N
NBoc2
O
O
B
O
O
Compound 6
Water
DMSO
0.99
1.95
2.08
0.93
1.00
0.97
1.96
2.08
3.06
18.67
11.09
17.71
10.0 9.5 9.0 8.5 8.0 7.5 7.0 6.5 6.0 5.5 5.0 4.5 4.0 3.5 3.0 2.5 2.0 1.5 1.0 0.5 0.0
f1 (ppm)
1d_C13 DMSO E:\\ kost-ts 37
161.70
158.95
156.20
150.26
149.10
149.01
146.39
140.60
134.50
130.35
129.83
126.81
120.71
113.81
112.97
83.62
83.32
83.13
69.70
55.33
27.29
27.10
24.64
DMSO
200 190 180 170 160 150 140 130 120 110 100 90 80 70 60 50 40 30 20 10 0
f1 (ppm)

190220-Hassanpour-SH…….. 02/20/19 16:00:32

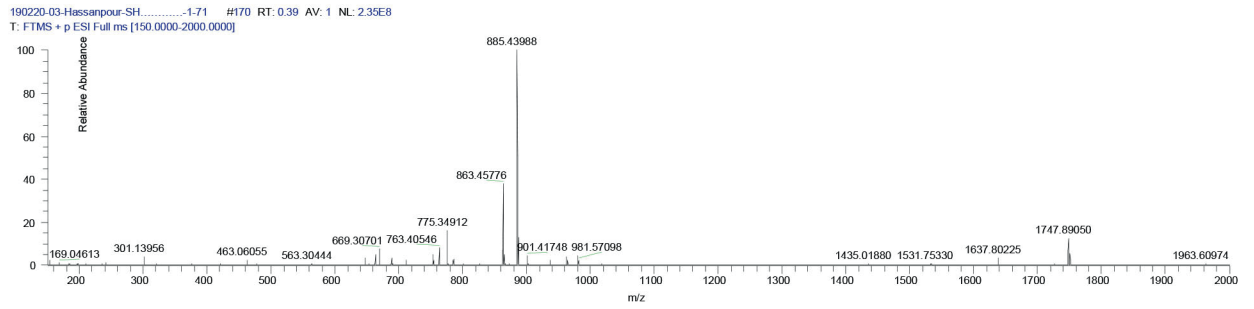


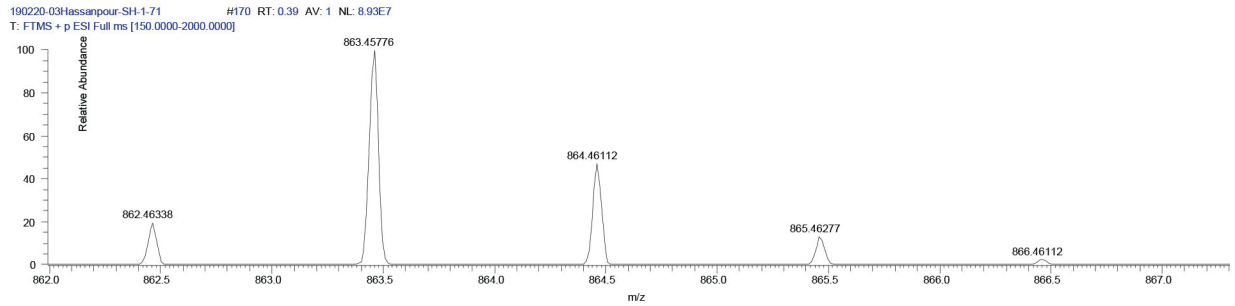


190220-03Hassanpour-SH-1-71 #170 RT:0.39
T:FTMS + p ESI Full ms [150.0000-2000.0000]
m/z= 863.40840-863.49407

| m/z | Intensity | Relative | Resolution | Charge | Theo. Mass | Delta (ppm) | RDB equiv. | Composition |
|---|---|---|---|---|---|---|---|---|
| 863.45776 | 91050248.0 | 100.00 | 19106.00 | 1.00 | 863.46083 | -3.55 | 16.5 | $C_{45}H_{64}O_{12}N_4B$ |

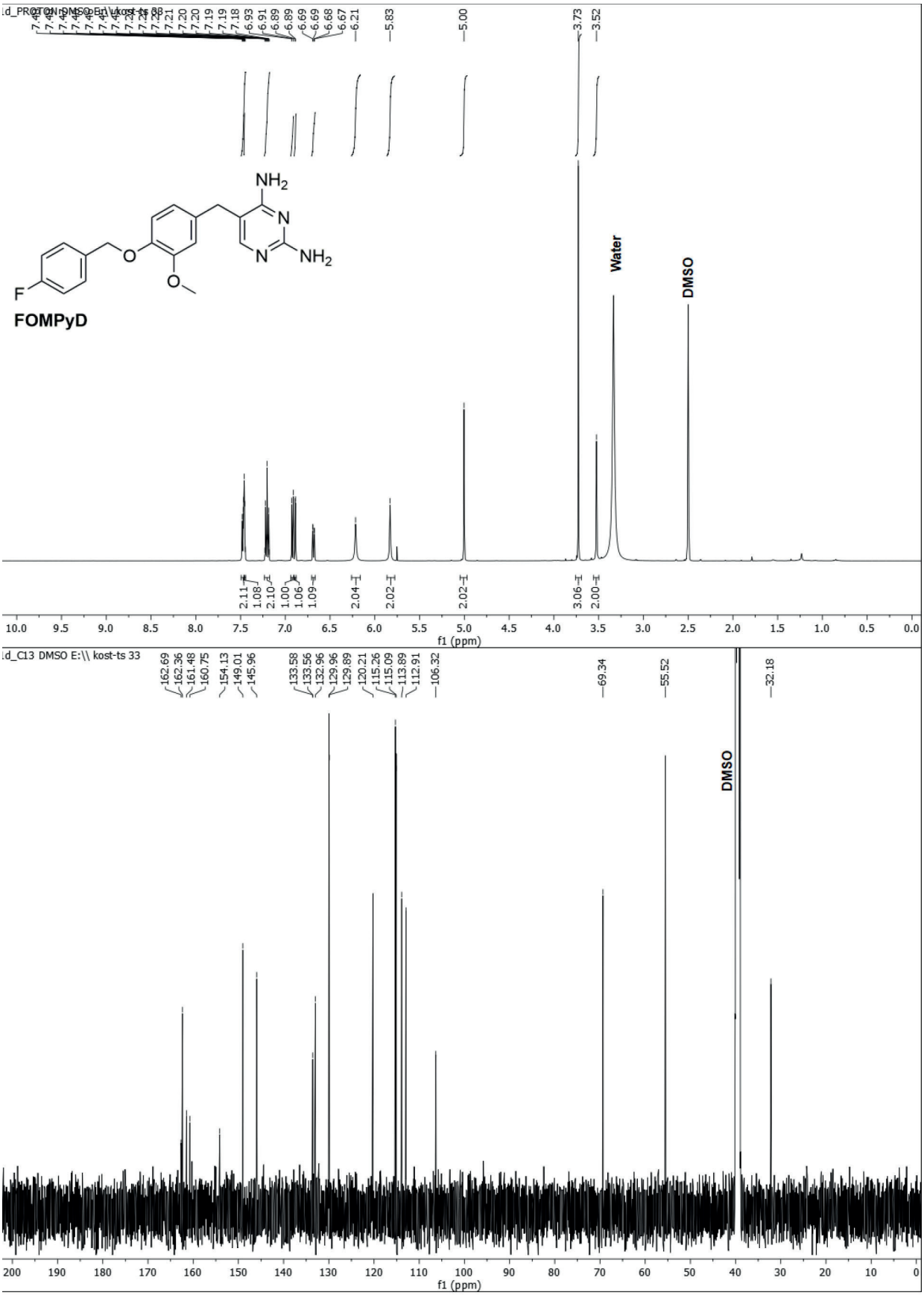
NH2
N
N
NH2
O
O
F
FOMPyD
Water
DMSO
f1 (ppm)
DMSO
f1 (ppm)

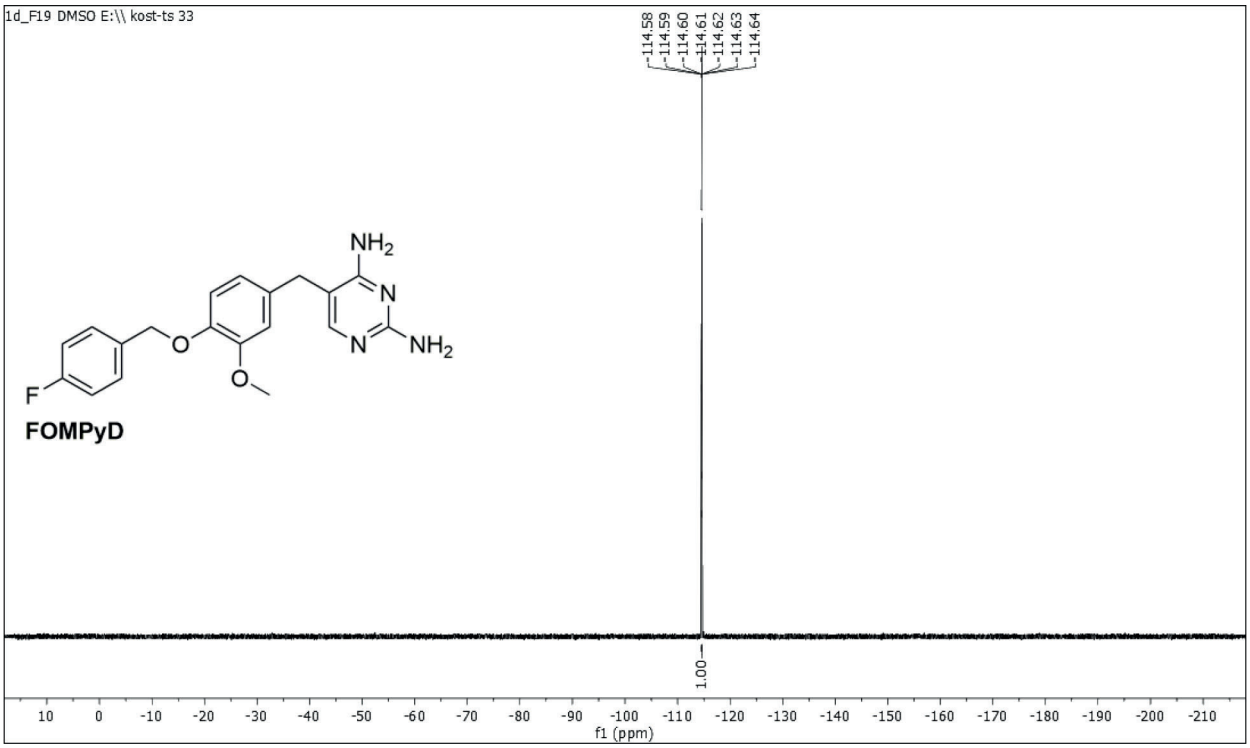


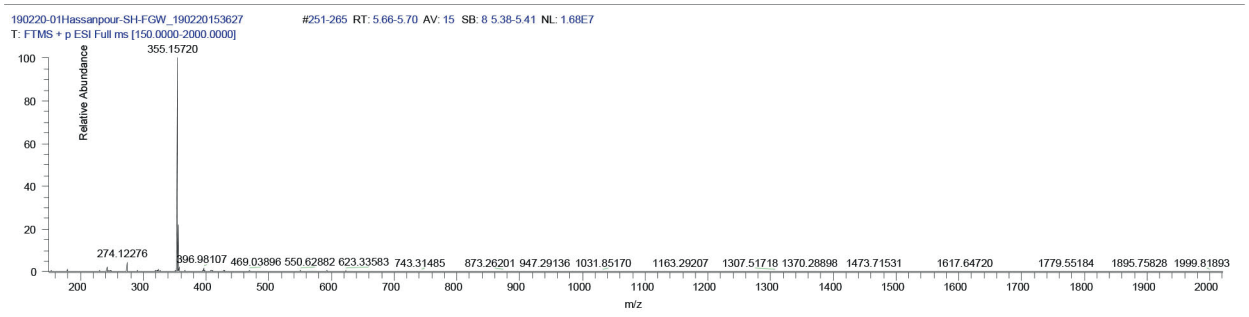


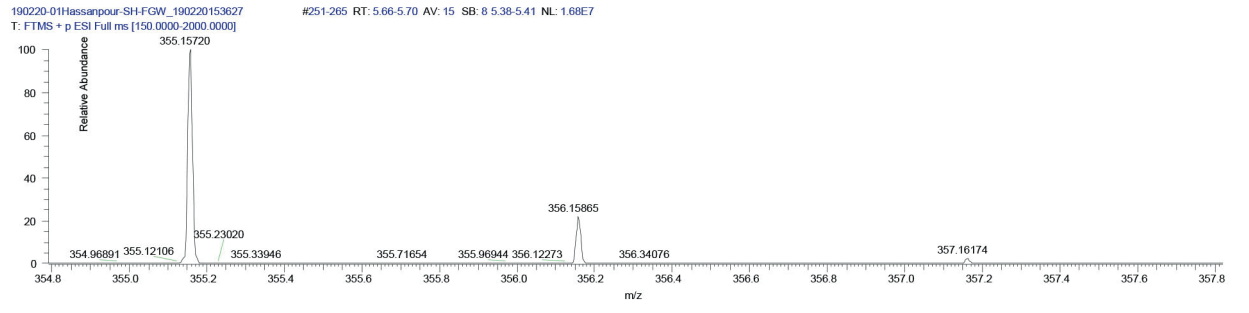


190220-01Hassanpour-SH-FGW_190220153627 #251-265 RT: 5.66-5.70 AV: 15
SB: 8 5.38-5.41
T: FTMS + p ESI Full ms [150.0000-2000.0000]
m/z= 355.13292-355.17932

| m/z | Intensity | Relative | Resolution | Charge | Theo. Mass | Delta (ppm) | RDB equiv. | Composition |
|---|---|---|---|---|---|---|---|---|
| 355.15720 | 17360554.0 | 100.00 | 27328.01 | 1.00 | 355.15782 | -1.75 | 11.0 | $C_{21}H_{22}O_3NF$ |
| | | | | | 355.15648 | 2.03 | 11.5 | $C_{19}H_{20}O_2N_4F$ |


Compound 7
Water
DMSO
f1 (ppm)
1d_C13 DMSO E:\\ kost-ts 6
DMSO
f1 (ppm)

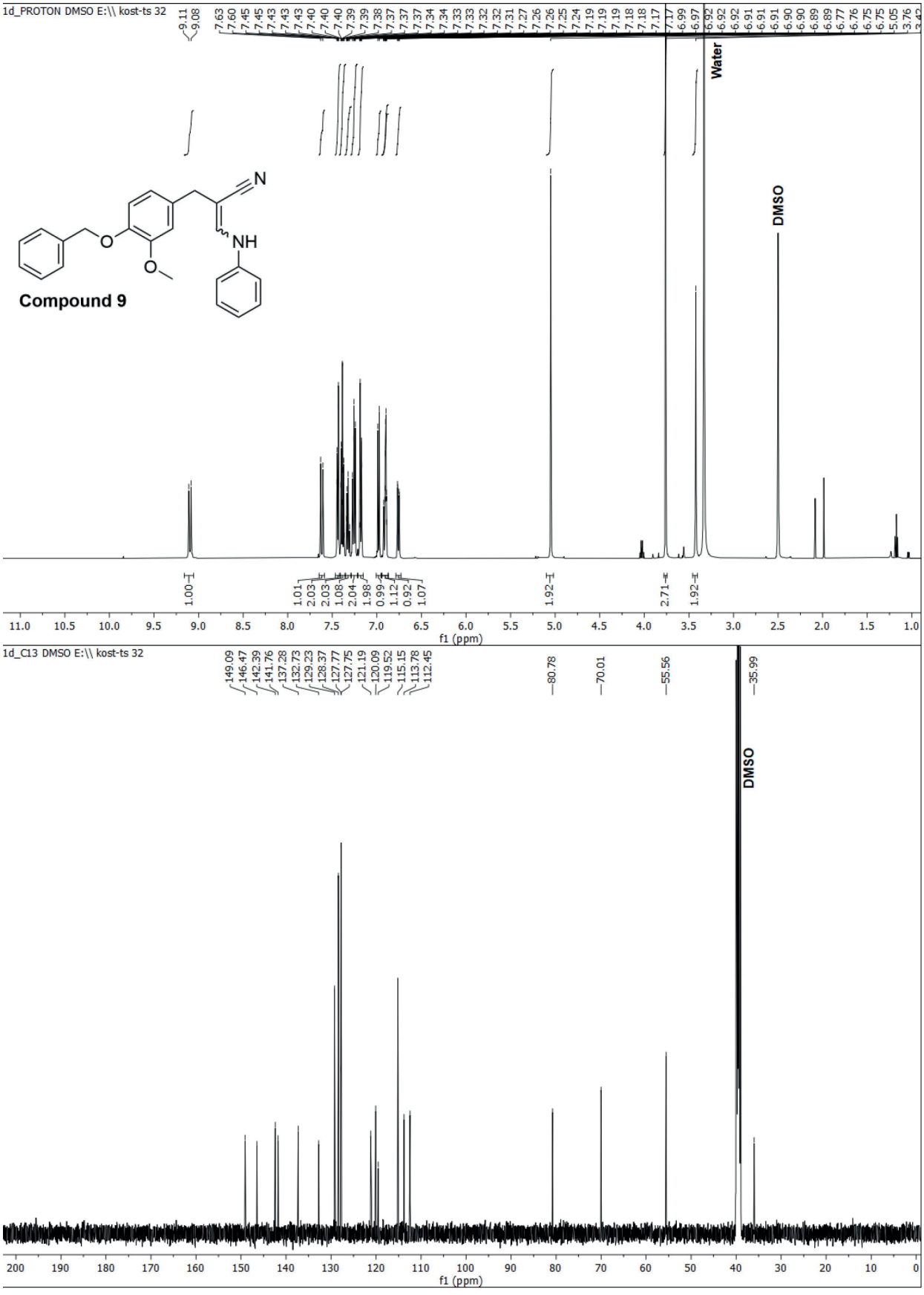
1d_PROTON DMSO E:\\ kost-ts 32
Water
DMSO
Compound 9
f1 (ppm)
1d_C13 DMSO E:\\ kost-ts 32
DMSO
f1 (ppm)

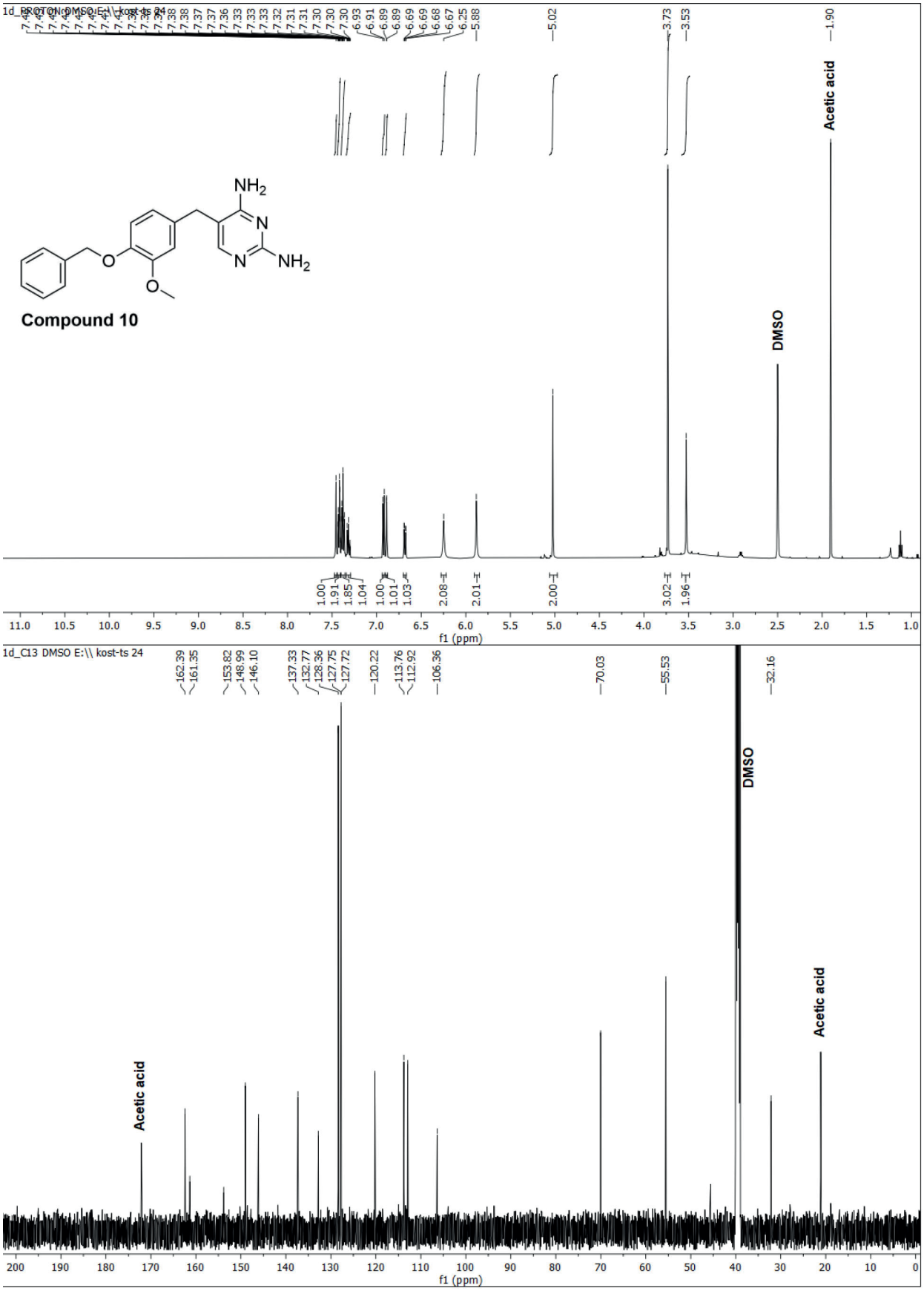
1d_PROTON DMSO E:\\ kost-ts 24
Acetic acid
DMSO
Compound 10
f1 (ppm)
1d_C13 DMSO E:\\ kost-ts 24
Acetic acid
DMSO
Acetic acid
f1 (ppm)

## 2. HPLC data

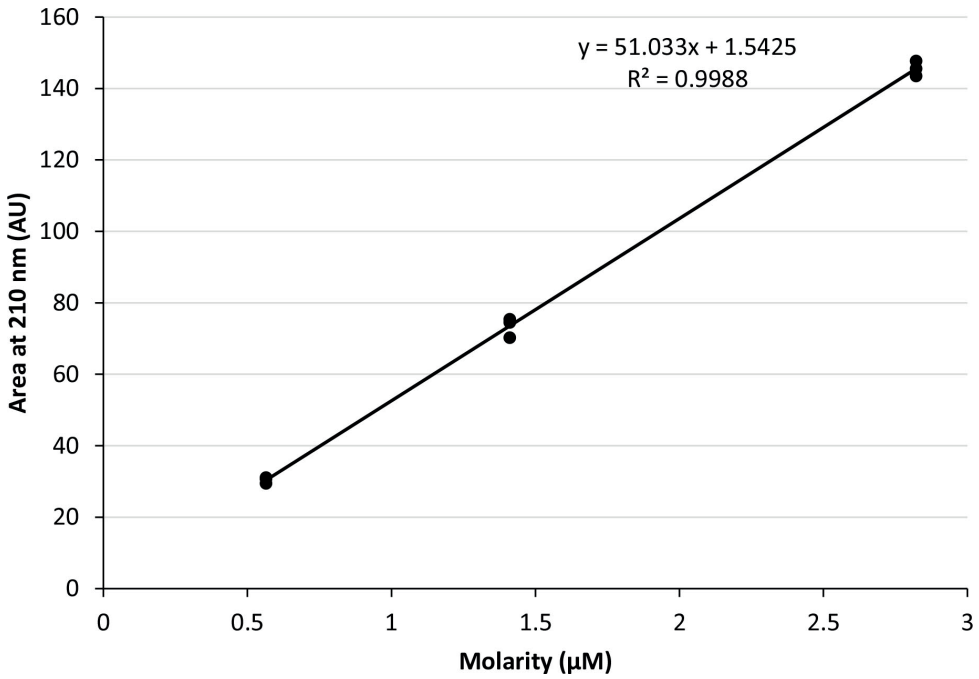


***Figure S1.*** *HPLC calibration curve of FOMPyD cold standard.*

## 3. Radio-TLC data

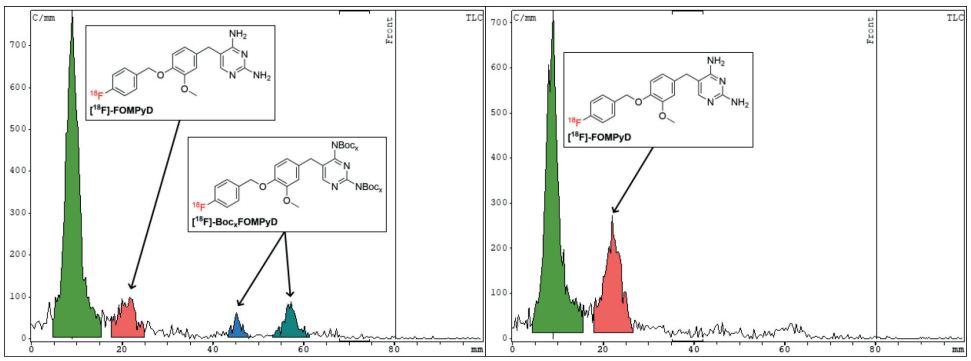


***Figure S2.*** *Radio-TLC trace of [18F]FOMPyD. (a) 10 minutes at 110°C, 23% 18F incorporation, 11% as [18F]BocxFOMPyD (x = 1 – 4); (b) 20 minutes at 110°C plus 10 minutes at 130°C, 26% 18F incorporation, <1% as [18F]BocxFOMPyD. TLC conditions: 10% MeOH/DCM.*

## 4. Supplemental autoradiography and MicroPET data

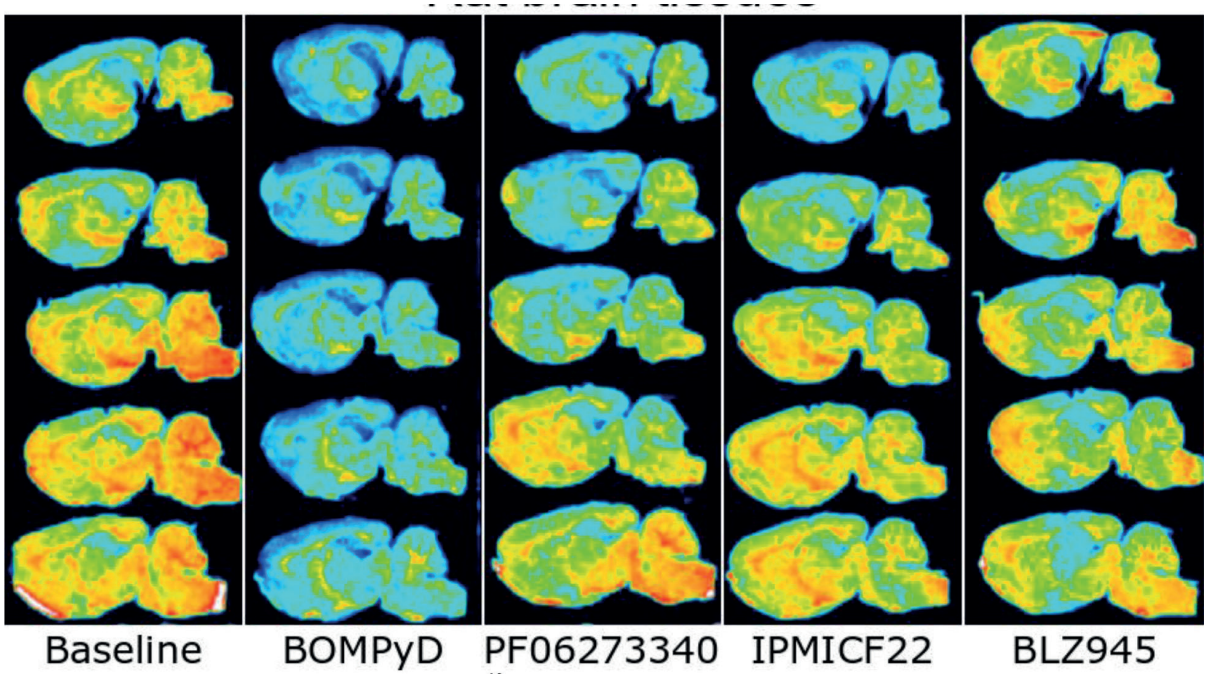


***Figure S3.*** *In vitro autoradiography investigation of 18F-FOMPyD on rat brain samples (0/02 mm) at the baseline by four various tyrosine kinase or Colony stimulating factor 1 receptor inhibitors (0/1 mM); see Figure S5 for the chemical structure of the blocking agent.*

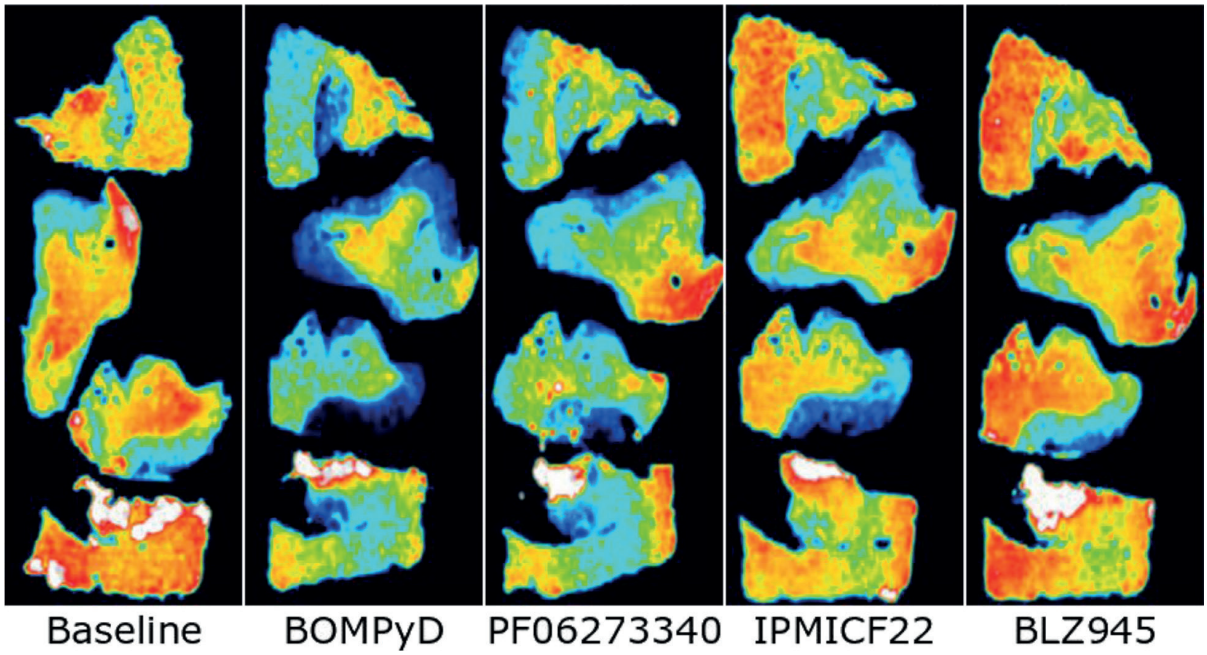


***Figure S4.*** *In vitro investigation of 18F-FOMPyD on human brain samples (posterior cingulate cortex, 0/02 mm) at the baseline by four multiple tyrosine kinase or Colony stimulating factor 1 receptor inhibitors (0/1 mM); see Figure S5 for the chemical structure of the blocking agent.*

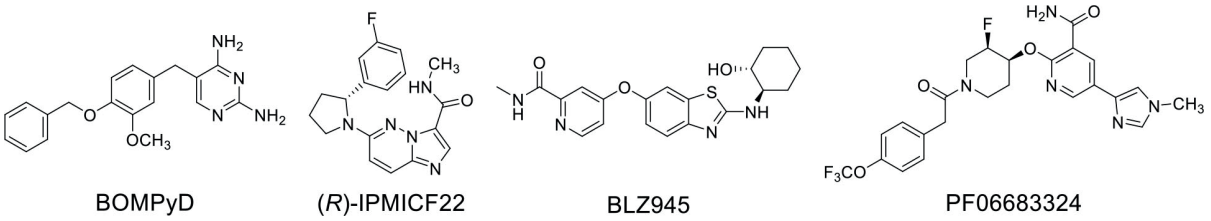


***Figure S5.*** *Chemical structures of blocking agents applied in this research.*

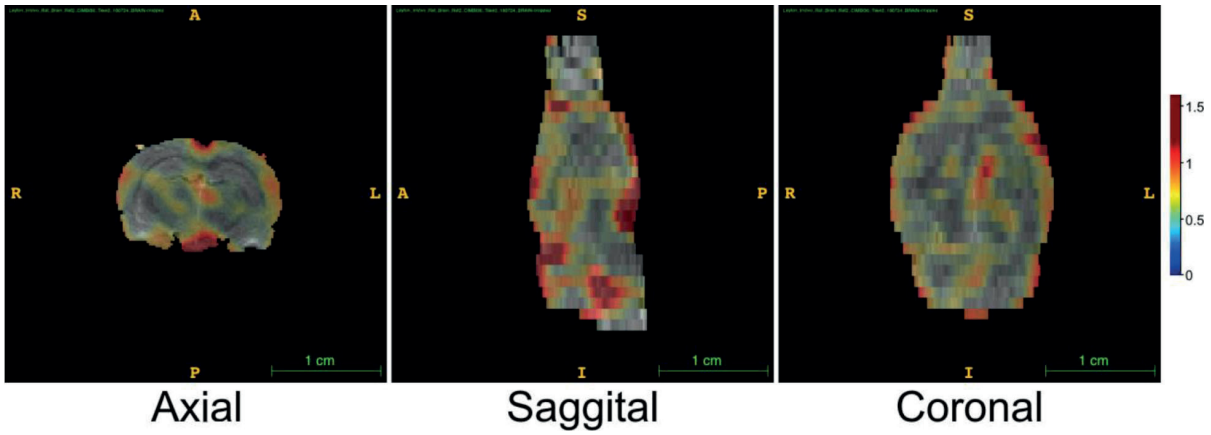


***Figure S6.*** *Figures indicate axial, sagittal, and coronal microPET slices of baseline the wild-type rat brain scans with 18F-FO-MPyD tracer, superimposed over an MRI image.*